WELLINGTON LUIZ DE ALMEIDA

PHOTOSYNTHETIC ACCLIMATION IN COFFEE IN RESPONSE TO WATER AVAILABILITY AND FRUITING: A HYDRAULIC AND HORMONAL APPROACH

Thesis submitted to the Plant Physiology Graduate Program of the Universidade Federal de Viçosa, in partial fulfilment of the requirements for the degree of the *Doctor Scientiae*.

VIÇOSA
MINAS GERAIS – BRASIL
2018

WELLINGTON LUIZ DE ALMEIDA

PHOTOSYNTHETIC ACCLIMATION IN COFFEE IN RESPONSE TO WATER AVAILABILITY AND FRUITING: A HYDRAULIC AND HORMONAL APPROACH

Thesis submitted to the Plant Physiology Graduate Program of the Universidade Federal de Viçosa, in partial fulfilment of the requirements for the degree of the *Doctor Scientiae*.

APPROVED: September 25, 2018.

_____
Auxiliadora Oliveira Martins

_____
Amanda Ávila Cardoso

_____
Samuel Cordeiro Vitor Martins
(Co-adviser)

_____
Dimas Mendes Ribeiro
(Co-adviser)

_____
Fábio Murilo da Matta
(Adviser)

Acknowledgements

Abbreviations

A: net photosynthesis rates (μmol CO_2 m^2 s^{-1});

ABA: abscisic acid;

ACC: 1-aminocyclopropane-1-carboxylic acid;

ANOVA: variance analysis;

C_a: ambient CO_2 concentration;

C_c: chloroplastic CO_2 concentration;

C_i: intercellular CO_2 concentration;

C_{leaf}: leaf capacitance (mol m^{-2} MPa^{-1});

C_{TLP}: leaf capacitance after the turgor loss point (mol m^{-2} MPa^{-1});
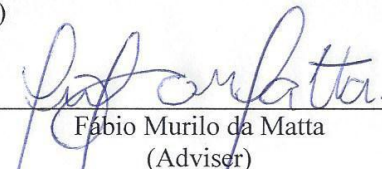
DM: dry mass (g);

E: transpiration rate (mmol H_2O m^2 s^{-1});

ETR: electron transport rate (μmol e- m^2 s^{-1});

F: fruited;

$F_{0'}$: initial fluorescence of the leaf tissue adapted to the light;

F_0: initial fluorescence;

$F_{m'}$: maximum fluorescence of the leaf tissue adapted to light;

F_m: maximum fluorescence;

F_s: steady-state fluorescence yield;

g_m: mesophyll conductance (mol CO_2 m^2 s^{-1});

g_s: stomatal conductance (mol H_2O m^2 s^{-1});

HSD: honestly significant difference.

I: irrigated;

IAA: indole-3-acetic acid;

K_{leaf}: leaf hydraulic conductance (mmol m^{-2} s^{-1} MPa^{-1});

K_{plant}: plant hydraulic conductance (mmol m^{-2} s^{-1} MPa^{-1});

l_b: biochemical limitations;

l_m: mesophyll limitations;

l_s: stomatal limitations;

MW: mass of water (g);

NF: non-fruited;

NI: non-irrigated;

NPQ: nonphotochemical quenching coefficient;

PAR: photosynthetically active radiation (µmol photons m^{-2} s^{-1});

q_P: photochemical quenching coefficient;

R: rainfall (mm H_2O d^{-1});

R_D: diurnal respiration (µmol CO_2 m^2 s^{-1});

R_d: mitochondrial respiration rate in the dark (µmol CO_2 m^2 s^{-1});

R_P/A_{gross}: photorespiration-to-gross photosynthesis ratio;

R_P: photorespiratory rate of RuBisCO (µmol CO_2 m^2 s^{-1});

RuBisCO: ribulose-1,5-bisphosphate carboxylase/oxygenase;

RWC: relative water content (%);

RWC_{TLP}: relative water content at the turgor loss point (%);

SLA: specific leaf area (mm^2 kg^{-1});

T_{air}: air temperature (°C);

V_{cmax}: maximum rate of carboxylation by RuBisCO;

VPD: leaf-to-air vapor pressure difference (MPa);

WSC: water saturated content (g);

Symbols

$\Delta\Psi$: leaf water potential difference between predawn and midday (MPa);

Ψ_{stem}: stem water potential (MPa);

Ψ_{md}: leaf midday water potential (MPa);

Ψ_{pd}: leaf predawn water potential (MPa);

$\Psi_{\pi(100)}$: osmotic potential at full turgor (MPa);

$\Psi_{\pi(TLP)}$: osmotic potential at the turgor loss point (MPa);

ε: bulk modulus of elasticity;

α: leaf absortance;

β: partitioning of electrons absorbed between the PSII and PSI.

ϕ_{PSII}: actual photosystem II quantum yield;

Abstract

ALMEIDA, Wellington Luiz de, D.Sc., Universidade Federal de Viçosa, September, 2018. **Photosynthetic acclimation of coffee in response to water availability and fruiting: A hydraulic and hormonal approach.** Adviser: Fábio Murilo da Matta. Co-advisers: Samuel Cordeiro Vitor Martins and Dimas Mendes Ribeiro.

The overall coordination between gas exchanges and plant hydraulics may be affected by the soil availability of water and source-to-sink relationships. Here we evaluated how coffee (*Coffea arabica* L. cv. Catimor) trees are able to acclimate their photosynthesis in response drought and fruiting. The plants, which were 6-yr-old at the beginning of trials, were grown in the field at full sunlight, and subjected to four treatment combinations: irrigated plants with fruits (I*F); irrigated plants with no fruits (I*NF); non-irrigated plants with fruits (NI*F) and non-irrigated plants with no fruits (NI*NF). A range of traits, encompassing from photosynthesis traits, water relations, growth and hormonal profile, were assessed. Over the course of the experiment, the non-irrigated plants displayed lower averaged values of predawn water potentials (-0.5 MPa) than their irrigated counterparts (-0.2 MPa). We showed that under mild water deficit conditions, irrigation *per se* did not impact growth rates but could reduce branch death significantly. These findings were unrelated to changes in leaf assimilate pools. We also demonstrated that fruiting provoked a feedforward effect on net photosynthesis rate that was fundamentally coupled to an enhanced stomatal conductance. Indeed both the mesophyll conductance and maximum rate of carboxylation by RuBisCO remained unchanged in response to the applied treatments. The increase in stomatal conductance was unrelated to varying abscisic acid levels or differential sensitivity to abscisic acid, although it was likely associated with a lower stomatal sensitivity to leaf-to-air vapor pressure difference. In parallel, the increases in transpiration rate were supported by coordinated alterations in plant hydraulics which should to a large extent explain the maintenance of plant water status regardless of fruiting-related variations in stomatal conductance and transpiration rate. In summary, we showed that stomatal conductance played a major role in the coordination between source capacity and sink demand regardless of irrigation, with concomitant changes in plant hydraulics. Therefore, these aspects should be considered in breeding programs to improve drought tolerance in coffee in face of the present and ongoing climate changes.

Resumo

ALMEIDA, Wellington Luiz de, D.Sc., Universidade Federal de Viçosa, setembro de 2018. **Aclimatação fotossintética do cafeeiro em resposta à disponibilidade hídrica e à frutificação: Uma abordagem hidráulica e hormonal.** Orientador: Fábio Murilo da Matta. Coorientadores: Samuel Cordeiro Vitor Martins e Dimas Mendes Ribeiro.

A coordenação geral entre as trocas gasosas e a hidráulica das plantas pode ser afetada pela disponibilidade de água no solo e pelas relações entre a fonte e o dreno. Aqui foi avaliado como árvores de café (*Coffea arabica* L. cv. Catimor) são capazes de aclimatar sua fotossíntese em resposta a seca e a frutificação. As plantas, com 6 anos de idade no início dos ensaios, foram cultivadas em campo a pleno sol e submetidas a quatro combinações de tratamento: plantas irrigadas com frutos (I*F); plantas irrigadas sem frutos (I*NF); plantas não irrigadas com frutos (NI*F) e plantas não irrigadas sem frutos (NI*NF). Uma série de características, incluindo características fotossintéticas, relações hídricas, crescimento e perfil hormonal, foi avaliada. No decorrer do experimento, as plantas não irrigadas apresentaram menores valores médios dos potenciais hídricos da madrugada (-0,5 MPa) do que suas contrapartes irrigadas (-0,2 MPa). Nós mostramos que, sob condições brandas de déficit hídrico, a irrigação, por si só, não impactou as taxas de crescimento, mas poderia reduzir significativamente a morte dos ramos. Esses achados não foram relacionados às mudanças nos pools de assimilação de folhas. Também demonstramos que a frutificação provocou um efeito de "feedforward" na taxa de fotossíntese líquida que foi fundamentalmente acoplado a uma melhor condutância estomática. De fato, tanto a condutância mesofílica como a taxa máxima de carboxilação pela RuBisCO permaneceram inalteradas em resposta aos tratamentos aplicados. O aumento na condutância estomática não foi relacionado com a variação dos níveis de ácido abscísico ou sensibilidade diferencial ao ácido abscísico, embora tenha sido provavelmente associado a uma menor sensibilidade estomática à diferença de pressão de vapor entre a folha e o ar. Paralelamente, os aumentos na taxa de transpiração foram suportados por alterações coordenadas na hidráulica da planta, o que deve explicar em grande parte a manutenção do "status" hídrico da planta, independentemente das variações relacionadas à frutificação na condutância estomática e na taxa de transpiração. Em resumo, mostramos que a condutância estomática desempenhou um papel importante na coordenação entre a capacidade da

fonte e a demanda do dreno, independentemente da irrigação, com mudanças concomitantes na hidráulica da planta. Portanto, esses aspectos devem ser considerados em programas de melhoramento genético para melhorar a tolerância à seca no café frente às atuais e atuais mudanças climáticas

Content

Introduction

Plants often face several harsh environmental conditions that potentially generate stresses. In particular, drought is by far the most important environmental constraint in agriculture. Hydraulic dysfunctions, caused by either soil water shortages or elevated vapor pressure differences between the leaf and the atmosphere (VPD), are well-known factors that can markedly impair leaf gas exchanges, and ultimately depressing growth and crop yields (Foley et al., 2011).

Leaf gas exchanges in higher plants is characterized by a dichotomy between the influx of CO_2 and the concomitant outflow of water vapor through the stomata pores, and therefore a trade-off between transpirational costs and CO_2 uptake is inherently inevitable. The CO_2 diffuses from the atmosphere to the intercellular air spaces and from there to the chloroplasts, where it is fixed by the activity of ribulose-1,5-bisphosphate carboxylase/oxygenase (RuBisCO). The CO_2 flux along this diffusional route is usually proportional to the stomatal conductance (g_s) and the mesophyll conductance (g_m) (Flexas et al., 2012). In fact, plants with higher net photosynthesis rates (A) usually exhibit greater values of g_s, g_m and transpiration rates (E). To support higher water demand, adjustments in plant hydraulics are required; overall, under optimum conditions, A is strongly correlated with g_s (and g_m) and leaf hydraulic conductance (K_{leaf}) (Santiago et al., 2004; Brodribb, 2009; Flexas et al., 2012; Flexas et al., 2013).

Coffee, an evergreen tropical tree species, is one of the most heavily globally traded agricultural commodities; it constitutes the social and economic basis of many tropical developing countries, with the livelihoods of 25 million smallholder farmers that depend on this crop (Waller et al., 2007). At current atmospheric CO_2 concentrations and saturating light, coffee leaves have low A, whose values typically vary from 4 to 11 μmol CO_2 m^{-2} s^{-1} which are within the lower range recorded for trees (DaMatta et al., 2018). However, the potential photosynthetic capacity of coffee leaves is relatively high (*ca.* 30 μmol CO_2 m^{-2} s^{-1}) and could be even greater than that of crops such as wheat and spinach, despite their low values of g_s and g_m (Martins et al., 2014). Indirect evidence suggests that the coffee's stomata are known to be highly sensitive to VPD (Batista et al., 2012) which is at least in part supposed to be

a consequence of intrinsically low K_{leaf} (Martins et al., 2014; Nardini and Luglio, 2014). Collectively, low values of g_s (and g_m) and K_{leaf} result in marked diffusive limitations with minor biochemical constraints to photosynthesis in coffee (Araujo et al., 2008; Martins et al., 2014; DaMatta et al., 2016). On the other hand, improved A via enhanced g_s has been registered under increased sink strength (e.g., high fruit loads) conditions (DaMatta et al., 2008; Ávila, 2016). For example, higher (>50%) A in fruiting branches than in their defruited counterparts has been observed (Franck et al., 2006; Ávila, 2016). However, the underlying mechanism by which an elevated sink demand exerts a feed-forward effect on coffee's photosynthesis via increases in g_s remains elusive.

In southeastern Brazil, a major region of coffee cropping, growth rates of the coffee tree are resumed in September with the first rains coupled with increased air temperatures, occasion where blossoming occurs. Vegetative growth rates are maximal from September/October through December when fruit dry mass accumulation is low, occurring the opposite from January through March when the coffee bean is filled. Thus, vegetative growth and fruit filling appear to occur at different times, suggesting incompatibility or competition between the two processes (see DaMatta (2018) for a review). Given that coffee beans are priority sinks, assimilate partitioning to them may be more than four-fold greater than that allocated to branch growth over the annual production cycle (Vaast et al., 2005).

Water shortages (and elevated VPD), which are common over the rainy season and are believed to become increasingly important due to the present and ongoing climate changes (DaMatta et al., 2018), have been empirically noted to depress plant growth; particularly when combined with high fruit loads, these shortages often lead to extensive branch death and tree degeneracy. It is possible that decreases in carbohydrate pools associated with lower A (due to decreased g_s) play key roles in this response. It should be emphasized that even mild water shortages are able to lead to decreases in g_s in coffee plants with concordant reductions in A (Dias et al., 2007; Menezes-Silva et al., 2017). These decreases, in turn, may be associated with enhanced levels of abscisic acid (ABA), the main hormone associated with stomata control; ABA can additionally trigger a signal cascade that leads to changes in both gene expression and leaf expansion and water stability (Vishwakarma et al., 2017). The anticipated decreases in g_s in a context of increased ABA levels may potentially constrain A regardless of fruiting burden. It remains to be investigated

how fruiting coffee trees deal with these dichotomous signs (i.e. decreases in g_s due to enhanced ABA levels under drought and increases in g_s due to fruiting) to optimize gas exchanges in the event of a drought stress.

Here we tested the following hypotheses: (i) irrigation improves growth rates and minimizes branch death in fruiting trees by allowing higher assimilate availability via improved photosynthetic performance; (ii) the feed-forward effect of fruiting on A via increases in g_s is coupled with an enhanced hydraulic performance to support E that unavoidably increases with the increasing g_s; (iii) this feed-forward effect reduces the stomata sensitivity to VPD, particularly in irrigated trees, due to the maintenance of K_{leaf}. To test these hypotheses, we designed a field experiment using integrative approaches combining measurements of branch (and leaf) growth and death, in-depth gas exchanges and water relations assessments, hormonal pools and some metabolites. We also assessed the stomata sensitivity to both ABA and VPD.

Material and Methods

Plant material, experimental design and growth conditions

The experiment was conducted under field conditions with coffee trees of cultivar 'Catimor', a hybrid derived from the cross between two cultivars: Caturra (*Coffea arabica* L.) and Timor (*C. arabica* x *C. canephora* Pierre ex Froehner). The plants, which were approximately 6 years old at the beginning of the trials, were grown as a hedgerow on a Red Yellowish Podzol in Viçosa (20°45'S, 42°15'W, 650 m in altitude), southeastern Brazil. The site is characterized by a subtropical climate with a mean annual temperature of 19 °C; it receives an average rainfall of 1,200 mm, which is mainly distributed from September/October to March (the growing season). The trees were cultivated in full sunlight and were planted at a spacing of 3.0 x 1.0 m. Routine agricultural practices for commercial coffee bean production, including hoeing, fertilization, and control of insect and pathogen attack, were used.

In mid-October 2016 (at the beginning of flowering), plants were divided into two groups, one of which had its flowers and bud flowers removed completely, and the other one remained with its full floral load, thus creating two fruiting treatments. Half of the fruited and defruited plants were continuously irrigated by

drip irrigation whereas the other half was grown without supplementary irrigation. Four treatments were therefore applied: irrigated plants with fruits (I*F); irrigated plants with no fruits (I*NF); non-irrigated plants with fruits (NI*F) and non-irrigated plants with no fruits (NI*NF). The treatments were distributed in a randomized complete block design with six replicates. Each block was performed as a row of 60 plants, and each experimental plot consisted of 10 plants; to avoid border effects, all sampling and field measurements were performed on the four central plants of each plot. Blocks were separated from each other by two rows of plants. Unless otherwise stated, all of the measurements and samplings (in leaves) were performed using the youngest, fully expanded leaves of the third or fourth pair from the apex of plagiotropic branches from the median third of the plant canopies. The meteorological data were extracted from an automatic station located at approximately 1 km from the experimental area (Code: 86824).

Vegetative growth and leaf expansion

Upon the application of treatments, the vegetative growth was biweekly evaluated by measuring the length and number of nodes of plagiotropic branches. The total branch length was measured with the aid of graduated rules positioned parallel to the previously selected plagiotropic branch. The number of nodes was also counted from a previously determined point. Four branches (two branches in each face of the hedgerow) were evaluated in each of the four useful plants, totalling 20 branches per plot. The rates of leaf expansion rate (LER), maximum time for leaf expansion and maximum leaf length were also evaluated in the second year of experiment. For this purpose, 20 leaves (1.0 ± 0.5 cm initial length) per plot, distributed in the middle third on both sides of the hedgerow, were periodically assessed by measuring their length and width until full leaf expansion. Leaf areas were then estimated using the maximum leaf widths and lengths, with the equations described by Antunes et al. (2008). Over the course of the experiment, the number of the previously selected branches that eventually died was recorded.

Water relations

The leaf water potential was measured at both pre-dawn (Ψ_{pd}) and midday (Ψ_{md}) on clear days using a Scholander type pressure pump (model 1000, PMS

4

Instruments, Albany, NY, USA). At pre-dawn, the leaves were collected and their water potentials were immediately measured. For the *in situ* Ψ_{md} measurements, leaves opposite to those used to measure Ψ_{md} were used to estimate Ψ_{stem}. The leaves used for the estimation of Ψ_{stem} were enclosed in a transparent plastic bag with an airtight closure (zip-lock) containing paper towel moistened in its interior and, later, wrapped with aluminium foil to guarantee the balance between the Ψ_{leaf} and the Ψ_{stem}. After measurements of Ψ_{md} on the uncovered leaves, the covered ones were stored in a hermetic polystyrene box to measure the water potential, which is supposed to correspond to Ψ_{stem} (Begg and Turner, 1970). Plant hydraulic conductance (K_{plant}) was calculated using the following equation (Nardini and Salleo, 2000):

$$K_{plant}= E/(\Psi_{pd}- \Psi_{md})$$

In which E is the transpiration rate (mmol H_2O m^2 s^{-1}) (estimated as described in the next session), is the Ψ_{pd} leaf water potential pre-dawn (MPa) and is the Ψ_{md} leaf water potential midday (MPa).

Pressure-volume curves (PV curves) were obtained as described elsewhere (Pinheiro et al., 2005; Cavatte et al., 2012) using leaves collected in the morning. Their petioles were immersed in distilled water for at least 8 h, after which the initial water potential (Ψ_0) was measured. Leaves with $\Psi_0 \leq$ -0.03 MPa were discarded. The leaves with appropriate Ψ_0 were then immediately weighed using a digital balance and lost water on the worktop before the Ψ_{leaf} and weight measured again. Measurements were repeated until the relation between the inverse of water potential and the relative water content (RWC) became strictly linear, which indicates that the turgor has been lost and, therefore, variations in the Ψ_{leaf} are only governed by changes in osmotic potential, that is, without contributions of the pressure potential. At the end of the measurements, leaves were dried at 70 °C until constant mass in order to obtain their dry masses. From the PV curves, the osmotic potential at full turgor ($\Psi_{\pi(100)}$) and at the turgor loss point ($\Psi_{\pi(TLP)}$), the RWC at the turgor loss point (RWC$_{TLP}$), saturated water content (SWC), leaf capacitance (C_{leaf}) and bulk modulus of elasticity (ε) were estimated (Cavatte et al., 2012). The WSC presented here was obtained by the ratio of water mass at saturation (estimated from the extrapolation between water mass (g) and water potential (MPa)) and leaf dry mass (g). The values of C_{leaf} were calculated from the beginning of the curvature of the relationship

between water potential (MPa) and RWC (%), expressed in absolute terms and normalized by leaf area, using the following equation:

$$C_{leaf} = \Delta RWC/\Delta \Psi_{leaf} \, (DW/LA) \, (MW/DW)/M$$

In which DW is the leaf dry weight (g), LA is leaf area (m^2), MW is the mass of leaf water at 100% of RWC (g) and M is the molar mass of water (g mol^{-1}). The values of leaf capacitance at full turgor (C_{leaf}) and after the turgor loss point (C_{TLP}) were obtained.

Gas exchanges and chlorophyll a fluorescence measurements

Gas exchange parameters were determined simultaneously with chlorophyll *a* fluorescence measurements under field conditions using a portable gas exchange system (LI-6400XT, LI-COR Inc., Lincoln, NE, USA) equipped with an integrated fluorescence chamber (LI-6400-40, LI-COR Inc.). The net CO_2 assimilation rate (A), the stomata conductance to water vapor (g_s) and the intercellular CO_2 concentration (C_i) were measured under a photosynthetically active radiation (*PAR*) of 1000 μmol photons m^{-2} s^{-1} at leaf level, and 400 μmol CO_2 mol^{-1} air. All of the measurements were performed at ambient temperature and VPD conditions, as described by DaMatta et al. (2016).

After recording the gas exchange parameters, the steady-state fluorescence yield (F_s) was measured after a pulse of saturating white light (8000 μmol m^{-2} s^{-1}; 0.8 s) that was applied to obtain the maximum fluorescence of the leaf tissue adapted to light (F_m'). The actinic light was turned off and a far-red illumination was applied (2 μmol m^{-2} s^{-1}) to measure the initial fluorescence of the leaf tissue adapted to the light (F_0'). Additionally, dark-adapted (30 min) leaf tissues were illuminated with weak modulated measuring beams (0.03 μmol m^{-2} s^{-1}) to obtain the initial fluorescence (F_0). Saturating white light pulses of 8,000 μmol photons m^{-2} s^{-1} were applied for 0.8 s to ensure for maximum fluorescence emissions (F_m). Using the values of these parameters, the photochemical quenching coefficient (q_P) and the nonphotochemical quenching coefficient (NPQ) were estimated (Maxwell and Johnson, 2000). The actual photosystem II quantum yield (ϕ_{PSII}) was determined following the procedures of Genty et al. (1989). The electron transport rate (ETR) was then calculated as ETR = ϕ_{PSII} β α *PAR*, where α is the leaf absorptance and β reflects the partitioning of

electrons absorbed between the PSII and PSI. We used the α β product determined for coffee by Martins et al. (2013).

The mitochondrial respiration rate in the dark (R_d) was measured at midnight and used to estimate diurnal respiration (R_D), according to Lloyd et al. (1995), as R_D = (0.5-0.05ln (PAR)) R_d. Corrections for temperature were performed using the temperature response equations from Sharkey et al. (2007). The photorespiratory rate of RuBisCO was calculated as R_P = 1/12 [ETR - 4 (A + R_D)], according to Valentini et al. (1995). Additional details can be found in DaMatta et al. (2016).

Five to seven A/C_i curves were obtained *in situ* (from approximately 08:00 to 12:00 h in February when g_s values were relatively elevated) from different plants per treatment. These curves were initiated at an ambient [CO_2] (C_a) of 400 μmol mol^{-1} air under a saturating PAR of 1,000 μmol m^{-2} s^{-1}. Once a steady state was reached, C_a was gradually decreased to 50 μmol mol^{-1} air. Upon the completion of the measurements at low C_a, C_a was returned to 400 μmol mol^{-1} air to restore the original A. Due to the intrinsically low g_s, particularly for the NI*NF plants (coupled to the negative g_s response to increases in C_a), we were unable to reliably estimate C_i at C_a values greater than 400 μmol mol^{-1}. Therefore, A/C_i curves only consisted of 7 different C_a values (≤400 μmol mol^{-1}). Corrections for the leakage of CO_2 into and out of the leaf chamber of the LI-6400 were applied to all gas exchange data as described by Rodeghiero et al. (2007). From the A/C_i curves, the maximum rate of carboxylation by Rubisco (V_{cmax}) based on a chloroplastic CO_2 concentration (C_c) and g_m was calculated using non-linear regression techniques based on Farquhar et al. (1980), and subsequently modified by Sharkey (1985) and Harley and Sharkey (1991). For this, the RuBisCO kinetic parameters were used as described above.

Finally, we estimated the overall photosynthetic limitations which were partitioned into their functional components [stomatal (l_s), mesophyll (l_m) and biochemical (l_b)], as described in Grassi and Magnani (2005)

VPD transition

The branches were harvested and brought to the laboratory in closed plastic bags containing moistened towel paper to minimize water loss through transpiration. The branches (totalling 6 per treatment) were recut in a container under deionized water, and then the gas exchanges were measured using the above-described infrared gas

analyser equipped with a conifer leaf chamber (6400-05, LI-COR Biosciences). In this chamber, the block temperature was maintained at 25 °C and the VPD was controlled by a portable dew point generator (LI-610, LI-COR Inc., Lincoln, NE, USA). After leaf enclosure, the initial VPD was adjusted to 1.0 ± 0.3 kPa, and the instantaneous gas exchanges were recorded every 30 s. After g_s reaching stability (approximately 10 min), the VPD was increased to 2.4 ± 0.5 kPa and so maintained until g_s was again held in check (approximately 10 min). The leaves were then removed from the chamber and immediately wrapped in moist paper towels, and bagged for 10 min (to allow the tissue balance) before measuring its water potential ($\Psi_{w\ Final}$) using a Scholander pressure chamber. The VPD was increased by passing the air entering through a desiccant (such treatment is faster than changing VPD using the dew point generator). The VPD was reduced by ignoring the desiccant column, returning the incoming air source directly to the dew point generator. Due to differences in the equilibrium time between the reference infrared gas analyser and samples (IRGAs), data obtained in the first 2 min immediately following the VPD transition were discarded. In order to estimate leaf water conductivity by the evaporative flow method (Sack and Scoffoni, 2012), the leaf opposite to that used in the VPD transition was enclosed in a transparent plastic bag with an airtight closure (zip-lock) containing moistened paper towels and then wrapped with aluminium foil; at the end of the VPD transition its water potential was measured to estimate the initial water potential ($\Psi_{w\ Initial}$). The K_{leaf} was estimated by the following formula:

$$K_{leaf} = E/(\Psi_{w\ Final} - \Psi_{w\ Initial})$$

ABA Sensitivity Curve

The branches were brought to the laboratory as described above. In the laboratory, the branch basis was recut in a container under a solution that stimulates stomata opening (5 mM KCl, 50 μM CaCl$_2$, 50 μM MES buffer diluted in distilled water; pH was adjusted to 6.15 using 1M TRIS buffer), and then a leaf was completely enclosed in a conifer chamber (6400-05, LI-COR Biosciences) that was attached to the above-mentioned infrared gas analyzer. The sizes of the branches were standardized at approximately 20 cm from their bases until the measured leaf. In the chamber, the block temperature was maintained at 25 °C and the VPD was controlled to 1.1 ± 0.5 kPa. The A, g_s and C_i were recorded at every 20 s measured under a *PAR*

of 1000 μmol photons m^{-2} s^{-1} at leaf level, and 400 μmol CO_2 mol^{-1} air. After g_s reaching stability (approximately 20 min), stock solution doses of ABA were applied to the opening solution in order to obtain the following final ABA concentrations: 0; 26; 132; 264; 660 ng mL^{-1}. The gas exchanges were measured until g_s again reached stability (approximately 60 ± 30 min). The leaves were removed from the chamber and immediately frozen in liquid nitrogen, and then stored at -80 °C until analysis for ABA quantification (see below).

Bioassay for stomata aperture

Stomata bioassays were performed according to the methodology described by Bright et al. (2006), with modifications. Leaf disks were floated with adaxial side up on the above-mentioned opening solution and incubated under a *PAR* of 150 μmol photons m^{-2} s^{-1} in Petri dishes at 25 °C for 2.0 h to allow stomata to open. The leaf disks were then treated with ABA at different concentrations supplemented in the same buffer opening medium for another 2.0 h. The disks were subsequently homogenized individually in approximately 100 mL of distilled water in a blender (Philips model RI2044, Brazil) for 30 s. The epidermal fragments were collected in 200 μm nylon mesh (Spectra-Mesh, BDH-Merck, Nottingham, UK) and transferred to a slide with one drop of distilled water and covered by a coverslip. The stomata openings of the epidermal fragments were then immediately measured using a calibrated light microscope (Model AX- 70 TRF, Olympus. Tokyo, Japan) coupled to an imaging system (Model Zeiss AxionCam HRc, Göttinger, Germany). In these images, stomata aperture was measured using the software Image-Pro® Plus (version 4.1, Media Cybernetics, Inc., Silver Spring, USA) Approximately 10 stomata were measured in each of the 12 replicates totalling 120 stomata per replicate ($n = 6$).

Hormonal profile

Hormones were extracted from 20 mg of lyophilized leaf material according to the methodology described by Müller and Munné-Bosch (2011), with modifications. 400 μL of extraction solution (methanol: isopropanol: acetic acid 20:79:1) were added after which the mixture was centrifuged (13,000 g, 10 min, 4 °C), and then 350 μL of supernatant were collected into a new tube. To the resulting precipitate, the extraction procedure was repeated and then added to the supernatants

obtained. In addition, a final centrifugation (20,000 g, 5 min at 4°C) was performed to remove traces of suspended tissues. Subsequently, the extract was injected (5 μL) into a liquid chromatograph (Agilent 1200 Infinity Series) coupled to the triple quadrupole mass spectrometry (QqQ) model 6430 (Agilent Technologies, Palo Alto, CA, USA) (LC-MS/MS). Chromatographic separation was performed on a Zorbax Eclipse Plus C18 column (1.8 μm, 2.1 x 50 mm, Agilent Technologies, Palo Alto, CA, USA) in series with a Zorbax protection column (SB C18, 1.8 μm, Agilent Technologies, Palo Alto, CA, USA). The mobile phase used consists of: (A) 0.02% acetic acid in water and (B) 0.02% acetic acid in gradient acetonitrile at a time of: 0/5; 11/60; 13/95; 17/95; 19/5; 20/5 s. A flow of 0.3 mL min^{-1} and a column temperature of 23 °C was used. Once in the mass spectrometer, the ESI (Electrospray Ionization) ion source was used with the following conditions: gas temperature of 300 °C, nitrogen flow rate of 10 L min^{-1}, nebulizer pressure 35 psi and capillary tension of 4000 V. Finally, the data generated were analysed in the "Skyline" program to obtain the peak area of each hormone in the samples, and the results were expressed in ng g^{-1} of lyophilized tissue.

Statistical analysis

First, the data were checked for a normality and homoscedasticity to verify whether they meet the ANOVA assumptions. Data on vegetative growth and leaf expansion were evaluated by three-way ANOVA for the following factors: fruiting (F and NF plants), irrigation (I and NI plants), sampling date, and their interactions. Death probability of branches was calculated for all treatment-combinations, and contrasted by χ^2 distribution (α=0.05). Data on gas exchanges, chlorophyll *a* fluorescence, metabolites, hormonal profile, and leaf water potentials were evaluated using a three-way ANOVA for the following factors: fruiting, irrigation and sampling dates (totalling 7 samplings), and their interactions. Variables from the PV curves, photosynthetic limitations and stomata aperture were evaluated using a two-way ANOVA for factors fruiting and irrigation. Relationship of g_s and foliar ABA levels measured for all treatment-combinations were adjusted using an exponential regression model (g_s=a·b$^{-(ABA)}$, α=0.05); in addition, the g_s was evaluated by one-way ANOVA. All of the comparisons between means were made using *a posteriori*

Tukey's HSD test (α= 0.05). All of the statistical analyses were performed with *R* programming language, version 3.5.1 (RCoreTeam, 2018).

Results

Environment and growth traits

Overall, air temperatures, VPD, and solar radiation were relatively high from early October through late March and low from early April through end August. Rains were much more abundant from November to December, especially in 2016, and short dry periods (5-12 days without precipitation) were common from January to March 2017. Overall, rains were less abundant from April until October 2017 (Supplementary Fig. 1).

Branch RGR was evaluated from late October 2016 through late June 2017. As expected, NF trees displayed higher RGR than their fruited counterparts regardless of irrigation (until late February), and the irrigation improved branch RGR in some periods but noticeably only in NF trees during the active growth phase (Fig. 1).

Fruits did not only affect branch RGR but also the area of an individual leaf which was, on average, 30% lower in fruiting trees than in NF ones, irrespective of irrigation. In any case, SLA was unresponsive to the treatments (Fig. 2).

Taking into account the evident competition between vegetative and reproductive growth we next decided to estimate the branch mortality probability (BMP) as a function of the applied treatments. The BMP increased in F trees but more markedly in I*NF trees (40%) in comparison with I*F trees (10%). In addition, branch death begun two months earlier in NI*F than in I*F plants (Fig. 3).

We also analyzed the leaf expansion rates (LER) in two periods: November-December 2017 (when vegetative growth peaks) and January-February 2018 (when reproductive growth peaks). Overall, fruiting, but not irrigation, affected LER and the final leaf size: LER was 23% and 48% higher, and final leaf size was 25% and 49% higher, in NF than in F trees, in the first and second periods, respectively (Fig. 4).

Water relations

As expected, water potentials (Ψ_{pd}, Ψ_{md} and Ψ_{stem}) were significantly lower in NI trees than in I trees regardless of fruiting. Values of Ψ_{pd} and Ψ_{md} averaged on -0.2 MPa / -1.2 MPa in I plants against -0.5 / -1.6 MPa in NI plants, respectively (Fig. 5A, B). The K_{plant} was significantly higher in I*F and lower in NI*NF trees, with intermediate values in I*NF and NI*F trees which did not differ to each other (Fig. 5). In turn, K_{leaf} was significantly lower (37%) in NI*NF trees than in trees from the other treatments (Fig. 6A). When comparing the I*F with NI*NF trees, Ψ_{s100} and Ψ_{s0}, and C_{leaf} all were higher (30, 18 and 39%, respectively) in the former, whereas the I*NF and NI*F individuals displayed values that did not differ significantly from those displayed by both the I*F and NI*NF trees (Fig. 6). The RWC_{TLP} and ε were unresponsive to the treatments (data not shown).

Hormonal profile

The leaf hormonal profile was evaluated in expanding leaves, at half its final size, in an attempt to show differences in hormonal pools that might explain differences in LER (Fig. 4). We also assessed the hormonal profile in mature leaves in three sampling dates (Supplementary Fig. 6). Regardless we did not find significant differences for ABA levels as well as for the other hormones or hormone precursors (jasmonic acid, salicylic acid, 1-aminocyclopropane-1-carboxylic acid, putrescine, spermidine, spermine, zeatin, indole-3-acetic acid).

Photosynthetic performance

Leaf gas exchange traits were assessed at both the early morning (07:30-08:30) and midday. Regardless of samplings, g_s (and *E*) and *A* were significantly higher in I*F and lower in NI*NF trees (on average, g_s = 101 mmol H_2O m^{-2} s^{-1} and *A* = 9.6 µmol CO_2 m^{-2} s^{-1} in I*F plants against 51 mmol H_2O m^{-2} s^{-1} and 5.6 µmol CO_2 m^{-2} s^{-1} in NI*NF plants), in contrast to the R_P/A_{gross} ratio which was lower in I*F and higher in NI*NF trees; the values of all of these traits were intermediate in I*NF and NI*F trees which did not differ to each other (Fig. 7). Overall, *A* displayed the highest values from January through March, period that coincides with the fruit filling phase (Fig. 7). Despite the differences in *A*, Chl *a* fluorescence traits (q_P, NPQ

and ETR) fluctuated minimally over the course of the experiment; on average, they were unresponsive to the treatments (Supplementary Fig. 3).

From the responses of A to CO_2 concentration, we found that both g_m and V_{cmax} did not change significantly among treatments so that differences in A should be almost entirely traceable by differences in g_s (Fig. 8). We next assessed the diffusional and biochemical components of the photosynthetic limitations relative to the I*F plants; we noted that l_m accounted for little, if at all, reductions in A whereas l_s was the main constraint of A, especially in NI*NF trees. The l_b also contributed to decrease A significantly, as noted in I*NF and NI*NF trees (Fig. 9).

Carbohydrates, amino acids and proteins

Despite some, if any, differences in the pools of carbohydrates (starch, sucrose, glucose and fructose), amino acids and proteins in some samplings, concentrations of these compounds were essentially similar, on average, among treatments (Supplementary Fig. 4 and 5).

VPD transition and stomatal sensitivity to exogenous ABA

During VPD transitions, g_s decreased markedly as VPD increased from 1.0 to 2.4 kPa. Regardless of irrigation, these decreases were less pronounced in F trees (averaged on 47%) when compared with their NF counterparts (averaged on 62%), although the rate of g_s reduction was unaffected by the treatments. Accordingly, A displayed the same pattern of response, with averaged decreases of 47% and 65% in F and NF trees, respectively (Fig. 11).

Irrespective of treatments, stomatal apertures, as assessed in isolated epidermis, decreased with the increasing ABA doses. Notably, greater values of maximum stomatal apertures (23%) were observed in F trees than in their NF counterparts. When applied an ABA dose equivalent to 26.32 ng mL^{-1} to the buffer solution stomatal aperture decreased by 43% (I*F plants) and by 49% (NI*NF plants), although apertures remained higher in epidermis from F plants (26%) than in those from NF plants. The values of g_s (leaves in excised branches, Fig.12) also decreased with the increasing ABA doses. Notably, greater values of maximum g_s (30%) were also observed in F trees than in their NF trees.

We tested the regression coefficients and found that both a and b coefficients were not significantly different among treatments indicating similar stomatal sensitivity to ABA.

Discussion

Irrigation did not improve vegetative growth rates, but markedly reduced branch death in fruiting trees

Here, we take the advantage of growing coffee trees under plantation conditions, and found that lack of irrigation produced a mild water deficit. However, we demonstrated that fruiting, but not irrigation, played the greatest role in explaining differences in vegetative growth rates.

Overall, the higher growth rates in NF trees than in F trees are in good agreement with previous studies on coffee under irrigated conditions (e.g.,Cannell, 1971; Amaral et al., 2001). Decreases in branch RGR during the active growth phase occurred from end-December onwards due possibly to increasing air temperature (Amaral et al., 2001). In any case, these decreases were more pronounced in F trees, which is believed to be a consequence of an exacerbated competition between vegetative and reproductive growth. Such a competition was particularly evidenced on the area of an individual leaf, which was smaller in F than in NF trees with no apparent effect of irrigation, especially when the leaf expanded during the phase of fruiting filling. The smaller leaves of F trees should reduce the gain of leaf area over the course of the active growth phase and thus affecting the source-sink relationships. In any case, the expected decreases in whole-plant leaf area in F plants could be at least in part compensated for the increase in *A* per unit leaf area (see below).

Differences in growth rates could not be explained by differences in carbohydrate and amino acid pools. Despite we have analyzed these pools in leaves, it has been reported that growing coffee trees may withdraw reserves from the root-trunk system and leaves concurrently (Nutman, 1932; Wormer and Ebagole, 1965). Anyhow, even when there were variations in carbohydrate levels (e.g., starch that was higher in NF than in F trees in January/early February), they were not apparently large enough to have significantly contributed to the differences in growth rates. In a previous study, Amaral et al. (2001) observed (irrigated conditions) higher growth

rates of NF trees than their F counterparts that were accompanied by higher leaf starch pools. Later studies, however, found no relationship between starch or sugar pools in leaves with differences in vegetative growth rates in response to varying source-to-sink ratios (DaMatta et al., 2008; Chaves et al., 2012), in agreement with this present report. In any case, all of these relationships should be considered with caution given that growth necessarily encompasses complex physiological and morphological alterations over time whilst instantaneous assessments of carbohydrate pools from single leaves express a momentary plant carbon balance.

Differences in LER and final leaf size were not accompanied by concordant alterations in the levels of hormones, such as ABA, which is known to affect leaf expansion (Chater et al., 2014). Indeed, the expanding leaves had, on average, higher (254%) levels of ABA than the expanded leaves. It has been reported that ABA from mature leaves is directed to the expanding ones, which would explain this discrepancy (Chater et al., 2014). These authors also pointed out that high concentrations of ABA in young leaves serve to positively regulate hydraulics and aquaporin activity to maximize cell expansion rate and facilitate leaf growth. However, our results suggest that, for the present experimental conditions, even with differences in LER during the fruit filling phase, leaf growth was not apparently modulated by leaf ABA levels.

In heavily-bearing coffee trees,, especially at full sun conditions, branch dieback is usually observed in coffee plantations (Vaast et al., 2005; Chaves et al., 2012). To the best of our knowledge, this study is the first report that quantitatively analyzed the mitigating effect of irrigation on branch death. However, in contrast to our working hypothesis, decreased branch death was apparently unrelated to the leaf pools of assimilates. In unirrigated coffee trees, Carvalho et al. (1993) and Chaves et al. (2012) also observed similar results. Here, we observed that F trees had higher E than their NF counterparts (see below). The smaller leaves in F trees might also create a higher boundary conductance, thus exacerbating plant transpiration. However, internal factors are also probably involved in this phenomenon given that I trees also displayed some branch dieback. In any case, by preventing branch death irrigation can contribute to decrease tree degeneracy in addition to avoiding biennial fluctuations in bean yields, thus concurring to improve sustainability of the coffee production chain.

Fruiting provoke a feed-forward effect in A via enhances in g_s regardless of irrigation

Our results clearly demonstrated a feed-forward effect of fruiting on *A*, in good agreement with previous studies on coffee (Ávila 2016; DaMatta et al., 2008). In other species, such as apple (Pretorius and Wand, 2003) and rice (Detmann et al., 2012), this effect has also been observed. Interestingly we showed that fruiting-related improvements on *A* took place even in NI trees. Given that our treatments did not cause significant changes in both g_m and V_{cmax} it can be suggested that the increases in *A* were fundamentally associated with higher g_s, thus confirming the lower stomatal limitations of photosynthesis with fruiting. It is also unlikely that differences in *A* had been associated with end-product accumulation (a fact that would be expected with decreasing sink strength) given that there were minimal, if any, differences in the pools of carbohydrates and amino acids, even in NF trees. Possibly, the higher vegetative growth rates might have acted as a significant sink for assimilates or these assimilates could be stored in the root-trunk system so that the assimilates in leaves could be maintained at low levels. Other studies have demonstrated that the leaf pools of assimilates did not change markedly during the growing season regardless of varying sink strength linked to differences in fruit-to-leaf ratios (Chaves et al., 2012; DaMatta et al., 2008).

A reduction in *A* was not accompanied by concordant adjustments in leaf photochemistry in NI*NF trees, as denoted by maintenance of the fraction of absorbed light that is dissipated photochemically (estimated as q_P) or thermally (estimated as NPQ) as well as in the maintenance of ETR. In this regard, increases in the R_P/A_{gross} ratio in the NI*NF trees suggest that photorespiration should have acted as the main sink of the excess energy.

The enhanced g_s was associated with decreased stomatal sensitivity to ABA and VPD

In order to gain insights on the underlying mechanism associated with higher stomatal apertures in F trees, we first analyzed the hormonal profile at the beginning, middle and end of the fruit filling phase. Overall, for our experimental conditions, the endogenous ABA levels of leaves varied minimally across treatments and

therefore do not explain the feed-forward effect of fruiting on g_s. On the other hand, we produced novel evidence that the increased sink strength due to fruiting led to decreased stomatal sensitivity to VPD and ABA. Indeed, to the best of our knowledge, this is the first study to quantitatively examine the responses of gas exchanges to VPD (in coffee) and how they are affected by fruiting. This lower sensitivity to VPD in F trees should be particularly important to guarantee higher gas exchanges rates and thus higher assimilate availability in the afternoon when unfavorable atmospheric conditions greatly constrain photosynthesis in coffee (Batista et al., 2012).

Cellular turgor, VPD and ABA are correlated with the stomata response, thus sensitivity to VPD may be correlated with sensitivity to ABA (McAdam and Brodribb, 2016). We performed our analyses of stomatal sensitivity to both VPD and ABA under laboratory conditions using excised branches that were immersed in water. Under these circumstances (and taking into consideration the mild drought stress under the conditions of this study) it is possible that leaves have been hydrated almost completely and thus masking the potential effects of drought stress on the stomatal sensitivity to VPD and ABA. This might help to explain why I*F trees exhibited averaged higher g_s than NI*F trees under field conditions in contrast to what was observed under controlled conditions when both g_s and stomatal aperture were similar between these trees when the branches were treated with the opening buffer solution. In any case, we found similar ABA levels and g_s sensitivity to ABA across treatments, ruling out a possible role for this phytohormone in explaining the g_s behavior in the field. Therefore, a likely candidate to partially explain the higher g_s in I*F trees is a lower sensitivity to VPD (observed in the field and under laboratory conditions) that occurs independently from field ABA levels.

In summary, we provide novel evidence for coffee that not only reinforces the high co-ordination between source and sink, irrespective of irrigation, but also explains how g_s is modulated by fruiting through a lower sensitivity to VPD in F treatments, thus ultimately causing a feed-forward effect on *A*.

High gas exchanges rates were coordinated with adjustments in plant water relations

Despite the greater values of g_s and E in F trees than in NF ones within each irrigation treatment there were no significant changes in Ψ_{pd}, Ψ_{stem} and Ψ_{md} in response to fruiting. Given that ε (and the RWC_{TLP}) remained invariant it is tempting to suggest that a similar RWC would be also observed within each irrigation treatment regardless of fruiting. In any case, the higher E in F than in NF trees can be translated into higher water use rates which were supported by corresponding adjustments in plant hydraulics, in good agreement with our working hypothesis. For example, I*F trees exhibited higher K_{plant} coupled with higher C_{leaf} than their NI*NF counterparts, whereas NI*F trees displayed higher K_{plant} and K_{leaf} than NI*NF trees. Collectively, these adjustments should help to buffer variations in water potentials (Blackman and Brodribb, 2011) whereas preserving maintenance, within given limits, of E.   Thus, high E could only be kept at high rates if K_{plant} also remains relatively high and from a certain point decreases as the water potential becomes more negative (Sperry et al., 2002). This partly explains why g_s was higher in NI*F plants than in NI*NF ones under mild water deficit.

The lower K_{plant} and K_{leaf} in NI*NF trees should at least in part explain their lower g_s in addition to concurring to explain their sensitivity to VPD. In any case, these trees acclimated to water shortages via osmotic adjustment. Such an adjustment (not observed in the plants from the other treatments), which is associated with a net accumulation of solutes, can improve water uptake (Blum, 2017) and would act as a strategy for the NI*NF plants to cope with drought stress.

Conclusion

Here we showed that under mild water deficit conditions that are typical of most rainfed farms in the main Brazilian coffee producing area, irrigation per se did not impact growth rates but could reduce branch death significantly. These findings were unrelated to changes in leaf assimilate pools. We also demonstrated that fruiting provoked a feedforward effect on A that was fundamentally coupled to an enhanced gs. The increase in gs was unrelated to varying ABA levels although it was likely associated with a lower stomatal sensitivity to VPD. In parallel, the increases in E

were supported by coordinated alterations in plant hydraulics which should to a large extent explain the maintenance of plant water status regardless of fruiting-related variations in gs and E. In summary, we showed that gs played a major role in the coordination between source capacity and sink demand regardless of irrigation, with concomitant changes in plant hydraulics.

References

Ávila, RT. **Manipulation of source-to-sink ratios in girdled coffee branches evidences lack of photosynthetic down-regulation: the interplay of photosynthesis with respiration and photorespiration pathways and amino acid metabolism.** 2016. 47. Dissertação (Mestrado em Fisiologia Vegetal) - Universidade Federal de Viçosa, Viçosa, MG.

Amaral JAT, DaMatta FM, Rena AB (2001) Effects of fruiting on the growth of Arabica coffee trees as related to carbohydrate and nitrogen status and to nitrate reductase activity. Revista Brasileira de Fisiologia Vegetal. **13**: 66–74

Araujo WL, Dias PC, Moraes GABK, Celin EF, Cunha RL, Barros RS, DaMatta FM (2008) Limitations to photosynthesis in coffee leaves from different canopy positions. Plant Physiology and Biochemistry. **46**: 884–890

Batista KD, Araújo WL, Antunes WC, Cavatte PC, Moraes GABK, Martins SC V, DaMatta FM (2012) Photosynthetic limitations in coffee plants are chiefly governed by diffusive factors. Trees - Structure and Function **26**: 459–468

Begg JE, Turner NC (1970) Water potential gradients in field tobacco. Plant Physiology **46**: 343–346

Blackman CJ, Brodribb TJ (2011) Two measures of leaf capacitance: Insights into the water transport pathway and hydraulic conductance in leaves. Functional Plant Biology. **38**: 118–126

Blum A (2017) Osmotic adjustment is a prime drought stress adaptive engine in support of plant production. Plant, Cell & Environment. **40**: 4–10

Bright J, Desikan R, Hancock JT, Weir IS, Neill SJ (2006) ABA-induced NO generation and stomatal closure in Arabidopsis are dependent on H_2O_2 synthesis. The Plant Journal. **45**: 113–122

Brodribb TJ (2009) Xylem hydraulic physiology: The functional backbone of terrestrial plant productivity. Plant Science. **177**: 245–251

Cannell MGR (1971) Effects of fruiting, defoliation and ring-barking on the accumulation and distribution of dry matter in branches of *Coffea arabica* L. in Kenya. Australian Journal of Experimental Agriculture. **7**: 63–74

Carvalho CHS, Rena AB, Pereira AA, Cordeiro AT (1993) Relação entre a produção, teores de N, P, K, Ca, Mg, amido e a seca de ramos do catimor (*Coffea arabica* L.). Pesquisa Agropecuária Brasileira. **28**: 665–673

Cavatte PC, Oliveira AG, Morais LE, Martins SC V (2012) Could shading reduce the negative impacts of drought on coffee? A morphophysiological analysis. Physiologia Plantarum. **144**: 111-122

Chater C, Casson S, Gray JE, Chater CCC, Oliver J, Casson S, Gray JE (2014) Putting the brakes on : Abscisic acid as a central environmental regulator of stomatal development Tansley review Putting the brakes on : abscisic acid as a central environmental regulator of stomatal development. New Phytologist. **202**: 376-391

Chaves ARM, Martins SC V, Batista KD, Celin EF, DaMatta FM (2012) Varying leaf-to-fruit ratios affect branch growth and dieback , with little to no effect on photosynthesis, carbohydrate or mineral pools, in different canopy positions of field-grown coffee trees. Environmental and Experimental Botany. **77**: 207–218

DaMatta FM, Avila RT, Cardoso AA, Martins SC V, Ramalho JC (2018) Physiological and agronomic performance of the coffee crop in the context of climate change and global warming: A review. Journal of Agricultural and Food Chemistry. **66**: 5264–5274

DaMatta FM, Ramalho JD (2006) Impacts of drought and temperature stress on coffee physiology and production: A review. Brazilian Journal of Plant Physiology. **18**: 55–81

DaMatta FM, Godoy AG, Menezes-Silva PE, Martins SC V, Sanglard LMVP, Morais LE, Torre-Neto A, Ghini R (2016) Sustained enhancement of photosynthesis in coffee trees grown under free-air CO_2 enrichment conditions: Disentangling the contributions of stomatal, mesophyll, and biochemical limitations. Journal of Experimental Botany. **67**: 341–352

DaMatta FM, Ronchi CP, Maestri M, Barros RS (2008) Ecophysiology of coffee growth and production. Field Crops Research. **19**: 485–510

Detmann KC, Araújo WL, Martins SCV, Sanglard LMVP, Reis J V., Detmann E, Rodrigues FÁ, Nunes-Nesi A, Fernie AR, DaMatta FM (2012) Silicon nutrition increases grain yield, which, in turn, exerts a feed-forward stimulation of photosynthetic rates via enhanced mesophyll conductance and alters primary metabolism in rice. New Phytologist. **196**: 752–762

Dias PC, Araujo WL, Moraes GABK, Barros RS, DaMatta FM (2007) Morphological and physiological responses of two coffee progenies to soil water availability. Journal of Plant Physiology. **164**: 1639–1647

Farquhar GD v, von Caemmerer S von, Berry JA (1980) A biochemical model of photosynthetic CO_2 assimilation in leaves of C3 species. Plant. **149**: 78–90

Flexas J, Barbour MM, Brendel O, Cabrera HM, Carriquí M, Díaz-Espejo A, Douthe C, Dreyer E, Ferrio JP, Gago J, (2012) Mesophyll diffusion conductance to CO_2: An unappreciated central player in photosynthesis. Plant Science. **194**: 70–84

Flexas J, Niinemets Ü, Gallé A, Barbour MM, Centritto M, Diaz-Espejo A, Douthe C, Galmés J, Ribas-Carbo M, Rodriguez PL (2013) Diffusional conductances to CO_2 as a target for increasing photosynthesis and photosynthetic water-use-efficiency. Photosynthetic Research. **117**: 45–59

Foley JA, Ramankutty N, Brauman KA, Cassidy ES, Gerber JS, Johnston M, Mueller ND, O'Connell C, Ray DK, West PC (2011) Solutions for a cultivated planet. Nature. **478**: 337–342

Franck N, Vaast P, Génard M, Dauzat J (2006) Soluble sugars mediate sink feedback down-regulation of leaf photosynthesis in field-grown *Coffea arabica.* Tree Physiology. **26**: 517–525

Genty B, Harbinson J, Baker NR (1989) Relative quantum efficiencies of the two photosystems of leaves in photorespiratory and non-respiratory conditions. Plant Physiology and Biochemical. **28**: 1–10

Grassi G, Magnani F (2005) Stomatal, mesophyll conductance and biochemical limitations to photosynthesis as affected by drought and leaf ontogeny in ash and oak trees. Plant, Cell & Environment. **28**: 834–849

Harley PC, Sharkey TD (1991) An improved model of C3 photosynthesis at high CO_2: Reversed O_2 sensitivity explained by lack of glycerate reentry into the chloroplast. Photosynthetic Research. **27**: 169–178

Lloyd J, Grace J, Miranda AC, Meir P, Wong SC, Miranda HS, Wright IR, Gash JHC, McIntyre J (1995) A simple calibrated model of Amazon rainforest productivity based on leaf biochemical properties. Plant, Cell & Environment. **18**: 1129–1145

Martins SC V, Galmés J, Cavatte PC, Pereira LF, Ventrella MC, DaMatta FM (2014) Understanding the low photosynthetic rates of sun and shade coffee leaves: Bridging the gap on the relative roles of hydraulic, diffusive and biochemical constraints to photosynthesis. PLoS One. **9**: 1–10

Martins SCV, Galmés J, Molins A, DaMatta FM (2013) Improving the estimation of mesophyll conductance to CO2: On the role of electron transport rate correction and respiration. Journal of Experimental Botany. **64**: 3285–3298

Maxwell K, Johnson GN (2000) Chlorophyll fluorescence *a* practical guide. Journal of Experimental Botany. **51**: 659–668

McAdam SAM, Brodribb TJ (2016) Linking turgor with ABA biosynthesis: Implications for stomatal responses to vapor pressure deficit across land plants. Plant Physiology. **171**: 2008–2016

Menezes-Silva PE, Sanglard LMVP, Ávila RT, Morais LE, Martins SCV, Nobres P, Patreze CM, Ferreira MA, Araújo WL, Fernie AR, DaMatta FM

(2017) Photosynthetic and metabolic acclimation to repeated drought events play key roles in drought tolerance in coffee. Journal of Experimental Botany. **68**: 4309–4322

Müller M, Munné-Bosch S, Pan X, Welti R, Wang X, Dun E, Brewer P, Beveridge C, Davies P, Ross J (2011) Rapid and sensitive hormonal profiling of complex plant samples by liquid chromatography coupled to electrospray ionization tandem mass spectrometry. Plant Methods. **7**: 37

Nardini A, Luglio J (2014) Leaf hydraulic capacity and drought vulnerability: Possible trade-offs and correlations with climate across three major biomes. Functional Ecology. **28**: 810–818

Nardini A, Salleo S (2000) Limitation of stomatal conductance by hydraulic traits: Sensing or preventing xylem cavitation? Trees - Structure and Function. **15**: 14–24

Nutman FJ (1932) The root-system of *Coffea arabica* Pt. I. Root-systems in typical soils of british east Africa.

Pinheiro HA, DaMatta FM, Chaves AR, Fontes EPB, Loureiro ME (2005) Drought tolerance in relation to protection against oxidative stress in clones of Coffea canephora subjected to long-term drought. Plant science. **167**: 1307–1314

Pretorius JJB, Wand SJE (2003) Late-season stomatal sensitivity to microclimate is influenced by sink strength and soil moisture stress in "Braestar" apple trees in South Africa. Science Horticulture (Amsterdam). **98**: 157–171

Rodeghiero M, Niinemets Ü, Cescatti A (2007) Major diffusion leaks of clamp-on leaf cuvettes still unaccounted: How erroneous are the estimates of Farquhar et al. model parameters? Plant, Cell & Environment. **30**: 1006–1022

Sack L, Scoffoni C (2012) Measurement of leaf hydraulic conductance and stomatal conductance and their responses to irradiance and dehydration using the evaporative flux method (EFM). Journal of visualized experiments. **70**: 1–7

Santiago LS, Goldstein G, Meinzer FC, Fisher JB, Machado K, Woodruff D, Jones T (2004) Leaf photosynthetic traits scale with hydraulic conductivity and

wood density in panamanian forest canopy trees. Oecologia. **140**: 543–550

Sharkey TD (1985) Photosynthesis in intact leaves of C3 plants: physics, physiology and rate limitations. Botany reviewer. **51**: 53–105

Sharkey TD, Bernacchi CJ, Farquhar GD, Singsaas EL (2007) Fitting photosynthetic carbon dioxide response curves for C3 leaves. Plant, Cell & Environment. **30**: 1035–1040

Sperry JS, Hacke UG, Oren R, Comstock JP (2002) Water deficits and hydraulic limits to leaf water supply. Plant, Cell & Environment. **25**: 251–263

Vaast P, Angrand J, Franck N, Dauzat J, Génard M (2005) Fruit load and branch ring-barking affect carbon allocation and photosynthesis of leaf and fruit of Coffea arabica in the field. Tree Physiology. **25**: 753–760

Valentini R, Epron D, De Angelis P, Matteucci G, Dreyer E (1995) *In situ* estimation of net CO_2 assimilation, photosynthetic electron flow and photorespiration in Turkey oak (*Q. cerris* L.) leaves: diurnal cycles under different levels of water supply. Plant, Cell & Environment **18**: 631–640.

Vishwakarma K, Upadhyay N, Kumar N, Yadav G, Singh J, Mishra R, Kumar V, Verma R, Sharma S, Upadhyay RG (2017) Abscisic acid signaling and abiotic stress tolerance in plants: A review on current knowledge and future prospects. Frontiers in Plant Science. **8**: 161

Waller JM, Bigger M, Hillocks RJ (2007) Coffee pests, diseases and their management. CABI.

Wormer TM, Ebagole HE (1965) Visual scoring of starch in *Coffea arabica* L. II. Starch in bearing and non-bearing branches. Experimental Agriculture. **1**: 41–53

Figures
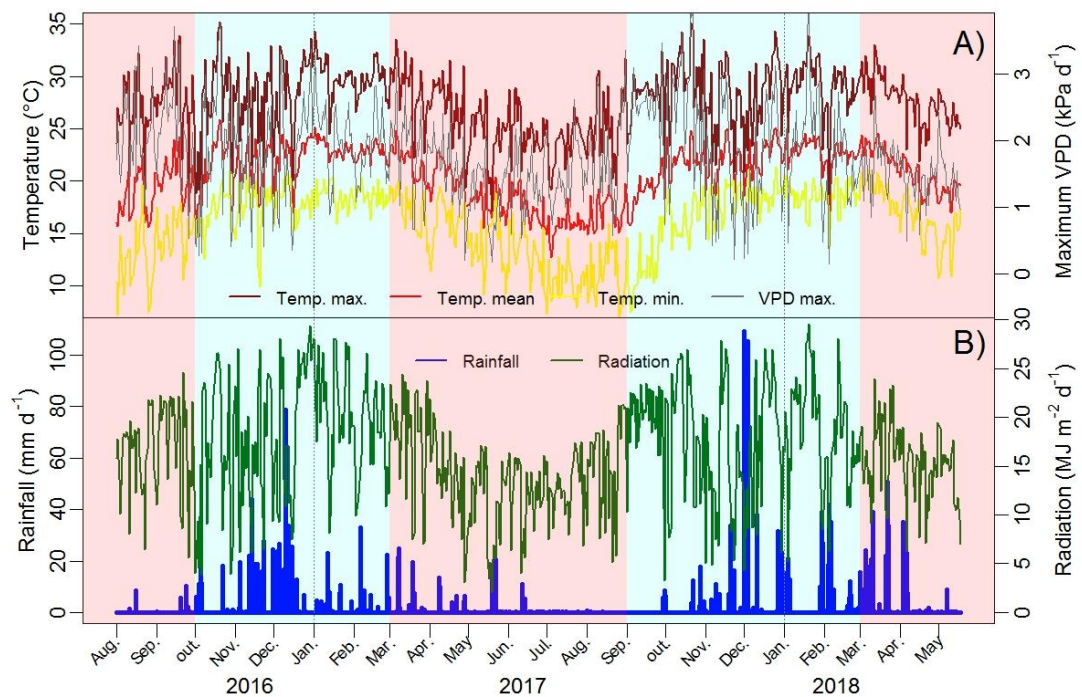
Supplementary Fig. 1. A) Time course of daily air temperature (maximum, mean, and minimum), and maximum vapour pressure deficit (VPD); B) daily rainfall and solar radiation. Blue area: period of active coffee tree growth; rose area: period of reduced coffee tree growth, from August 2016 through May 2018, in Viçosa, southeastern Brazil.
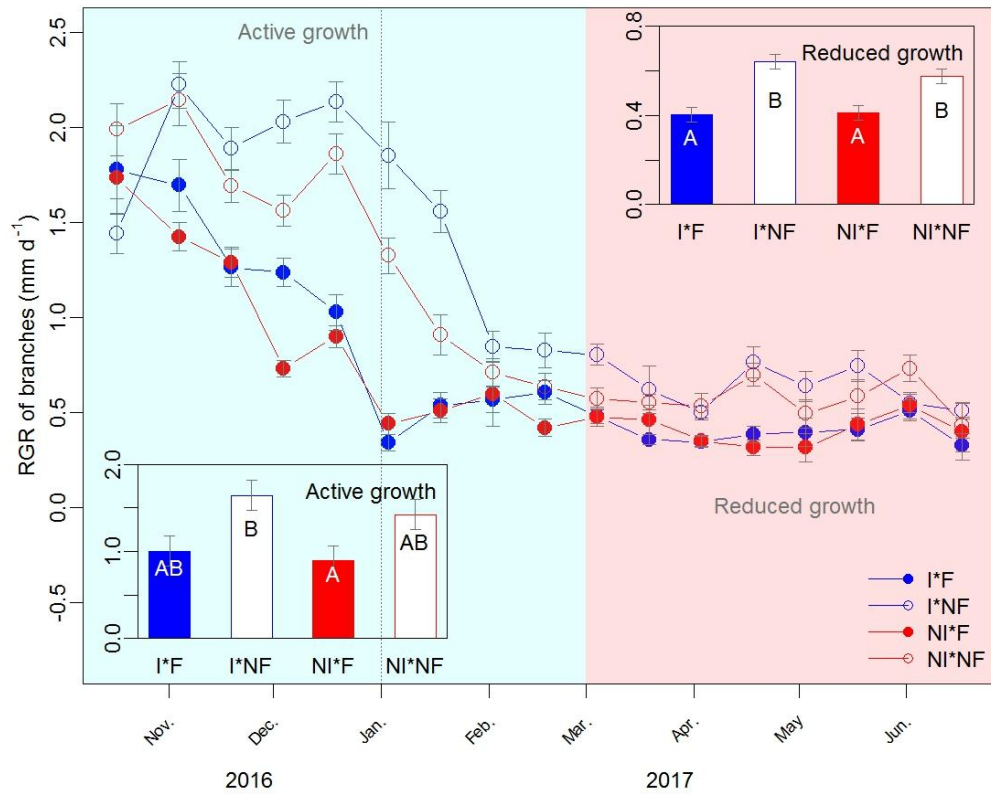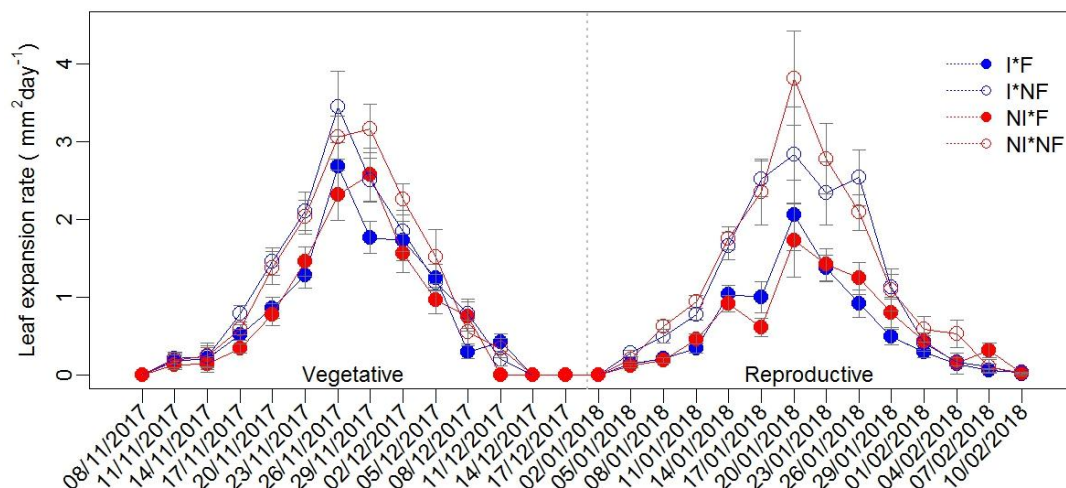
Fig. 1. Time course of relative growth rate (RGR) of branches of *Coffea arabica* trees grown in the field and subjected to four treatment combinations: irrigated plants with fruits (I*F); irrigated plants with no fruits (I*NF); non-irrigated plants with fruits (NI*F) and non-irrigated plants with no fruits (NI*NF) ($n = 20 \pm SE$). Vertical bars denote SE; when not shown, the SE was smaller than the symbols. Blue area: period of active coffee tree growth; rose area: period of reduced coffee tree growth. In the insets, mean values of RGR of branches over the course of the experiment are shown. Different letters indicate significant differences among between treatments, according to the Tukey HSD test, $p < 0.05$.
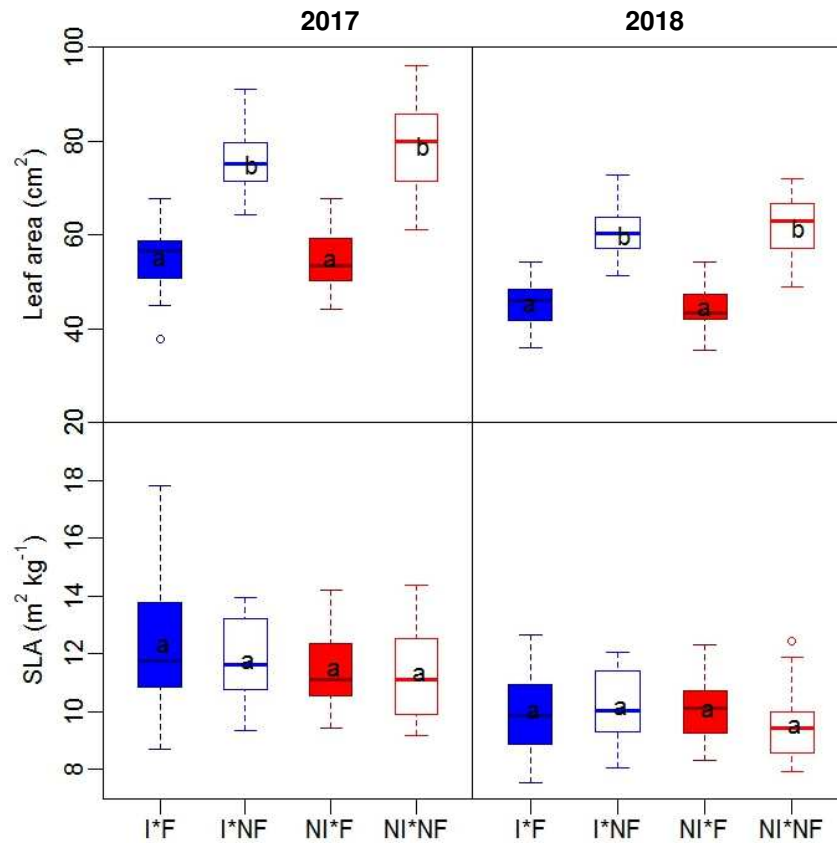
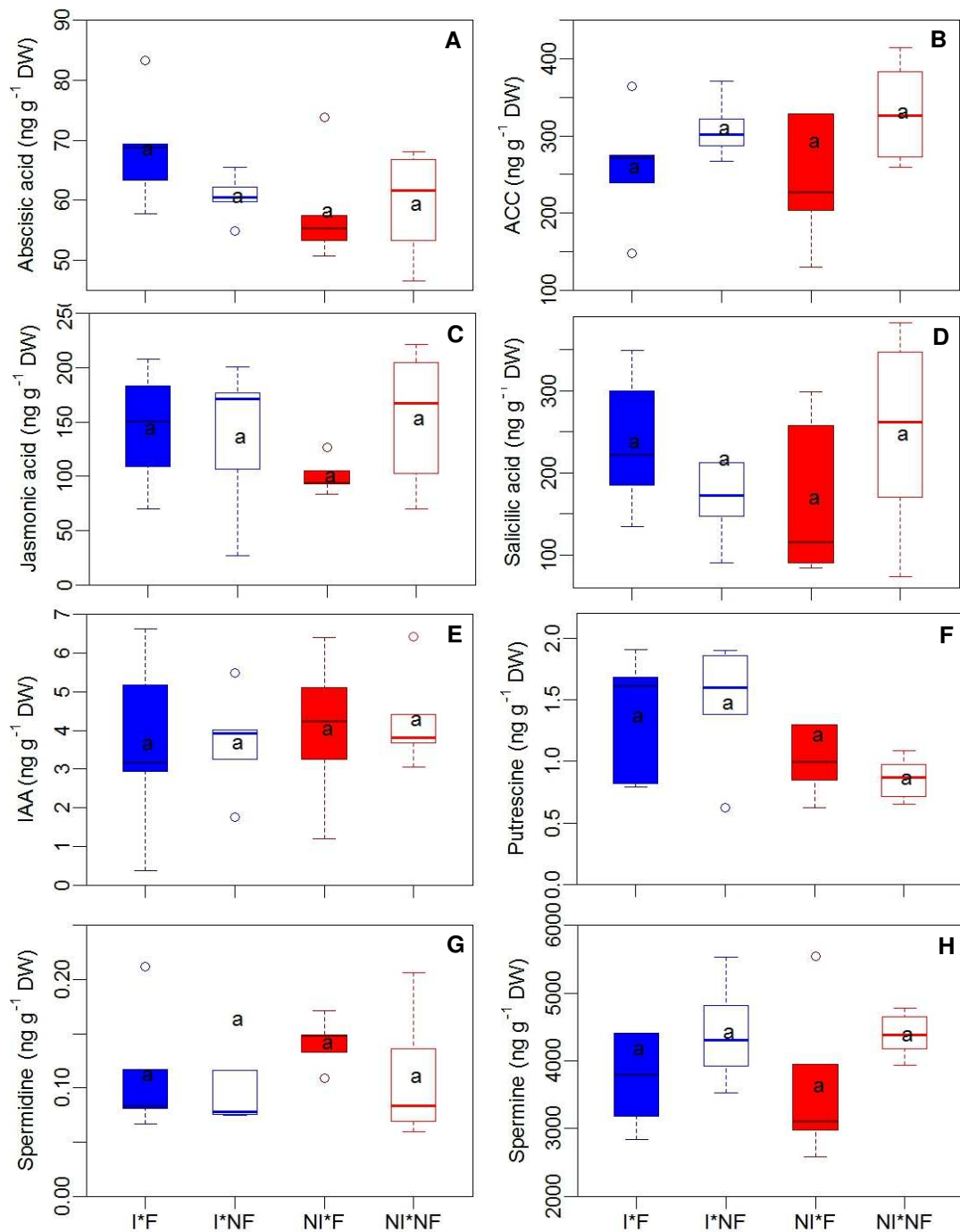**Fig. 2.** Leaf area and specific leaf area (SLA) in *Coffea arabica* trees grown in the field and subjected to four treatment combinations: irrigated plants with fruits (I*F); irrigated plants with no fruits (I*NF); non-irrigated plants with fruits (NI*F) and non-irrigated plants with no fruits (NI*NF) in January 2017 and January 2018 (*n* = 6). The xth percentile is the value below which x% of the observations are found. The lower and the higher part of the box indicate the 25th and 75th percentiles, respectively. The value of the bars are the 5th and the 95th percentile, and the 50th percentile (median) is given by the horizontal line within the box. Different letters indicate significant differences among between treatments, according to the Tukey HSD test, *p* < 0.05.
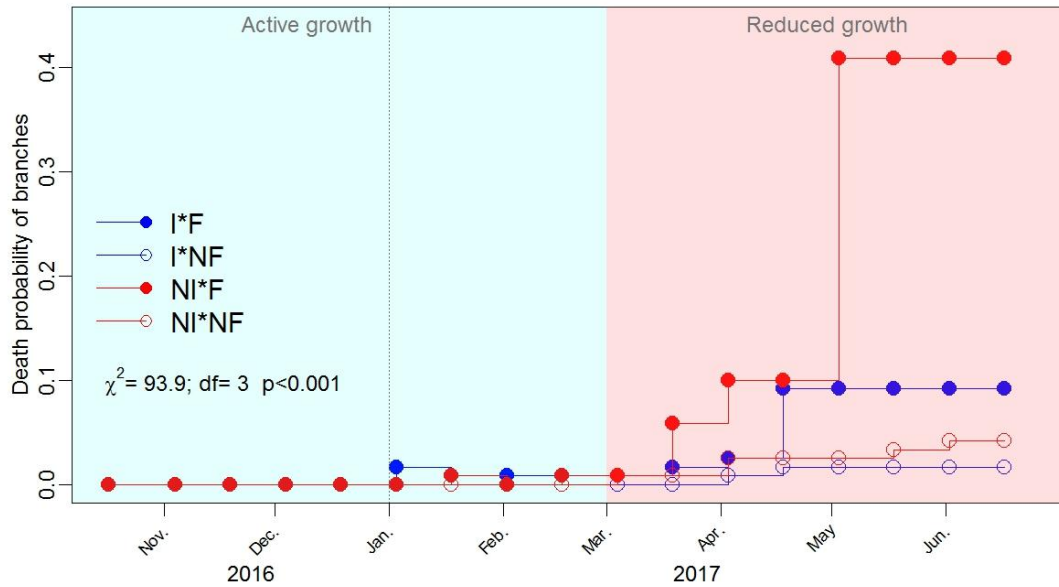
Fig. 3. Death probability of branches for *Coffea arabica* trees grown in the field and subjected to four treatment combinations: irrigated plants with fruits (I*F); irrigated plants with no fruits (I*NF); non-irrigated plants with fruits (NI*F) and non-irrigated plants with no fruits (NI*NF) (*n* = 20). Blue area: period of active coffee tree growth; rose area: period of reduced coffee tree growth. Death probability of branches was calculated for all treatment combinations, and contrasted by χ^2 distribution (α = 0.05).

Fig. 4. Time course of the foliar expansion rate of *Coffea arabica* trees grown in the field and subjected to four treatment combinations: irrigated plants with fruits (I*F); irrigated plants with no fruits (I*NF); non-irrigated plants with fruits (NI*F) and non-irrigated plants with no fruits (NI*NF), from November 2017 to February 2018. Each data point represents the mean value ($n = 20 \pm SE$). When not shown, the standard errors were smaller than the symbols.

Tab. 1. Maximum leaf area during leaf expansion and time for maximum expansion of *Coffea arabica* (as deduced from data from Fig. 4). Each value represents the mean value ($n = 20$). Different letters each column indicate significant differences among between treatments, according to the Tukey HSD test, $p < 0.05$.

|	Vegetative		Reproductive	
	Maximum leaf area (cm^2)	Time for maximum expansion (days)	Maximum leaf area (cm^2)	Time for maximum expansion (days)
I*F	34.10 a	39 a	24.19 a	37 a
I*NF	44.93 b	40 a	47.12 b	38 a
NI*F	33.39 a	37 a	25.27 a	42 a
NI*NF	46.77 b	39 a	52.27 b	40 a

Supplementary Fig. 2. The hormonal profile [A) Abscisic acid, B) 1-aminocyclopropane-1-carboxylic acid (ACC), C) jasmonic acid, D) indole-3-acetic acid (IAA) E) salicylic acid, F) putrescine, G) spermidine, H) spermine] as obtained in expanding leaves of *Coffea arabica* trees grown in the field and subjected to four treatment combinations: irrigated plants with fruits (I*F); irrigated plants with no fruits (I*NF); non-irrigated plants with fruits (NI*F) and non-irrigated plants with no fruits (NI*NF) ($n = 5$). The xth percentile is the value below which x% of the observations are found. The lower and the higher part of the box indicate the 25th and 75th percentiles, respectively. The value of the bars are the 5th and the 95th percentile, and the 50th percentile (median) is given by the horizontal line within the box. Different letters indicate significant differences among between treatments, according to the Tukey HSD test, $p < 0.05$.
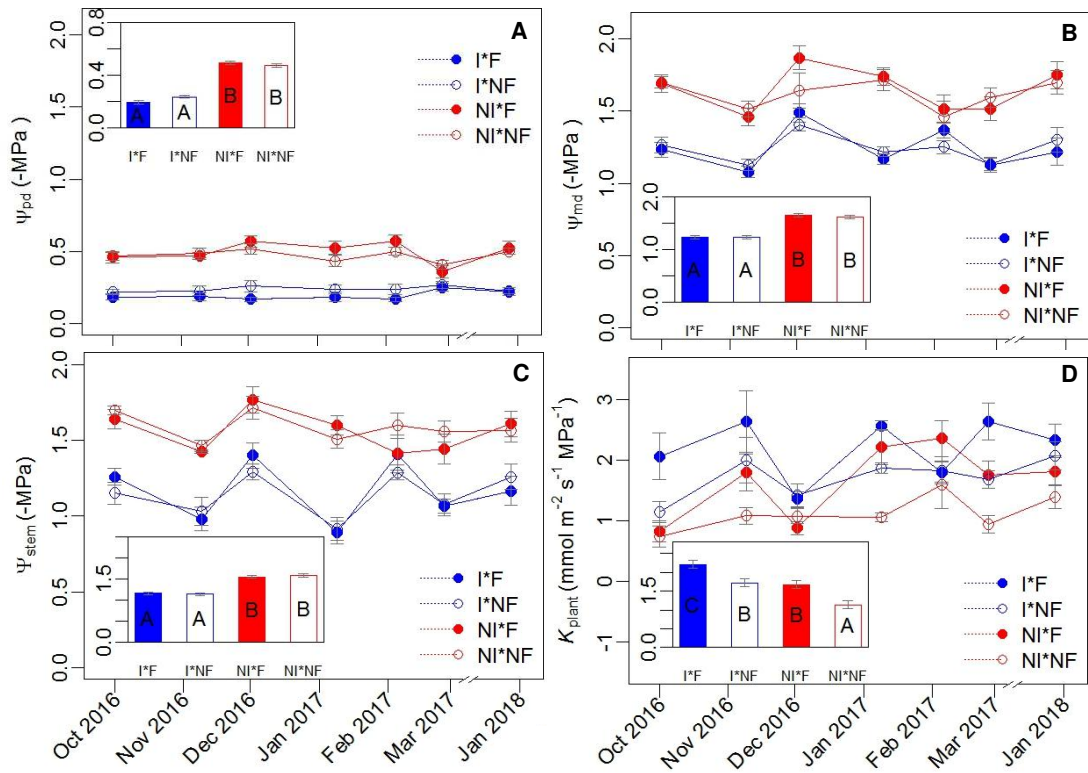
Fig. 5. Time course of leaf water potential at A) pre-dawn (Ψ_{pd}) and B) midday (Ψ_{md}), C) stem water potential (Ψ_{stem}) and D) plant hydraulic conductance (K_{plant}) in *Coffea arabica* trees grown in the field and subjected to four treatment combinations: irrigated plants with fruits (I*F); irrigated plants with no fruits (I*NF); non-irrigated plants with fruits (NI*F) and non-irrigated plants with no fruits (NI*NF), at 8:00h (left) and 12:00h (right) from October 2016 through January 2018. Each data point represents the mean value ($n = 6 \pm$ SE). Vertical bars denote SE; when not shown, the SE was smaller than the symbols. In the insets, mean values over the course of the experiment are shown. Different letters indicate significant differences among between treatments, according to the Tukey HSD test, $p < 0.05$.
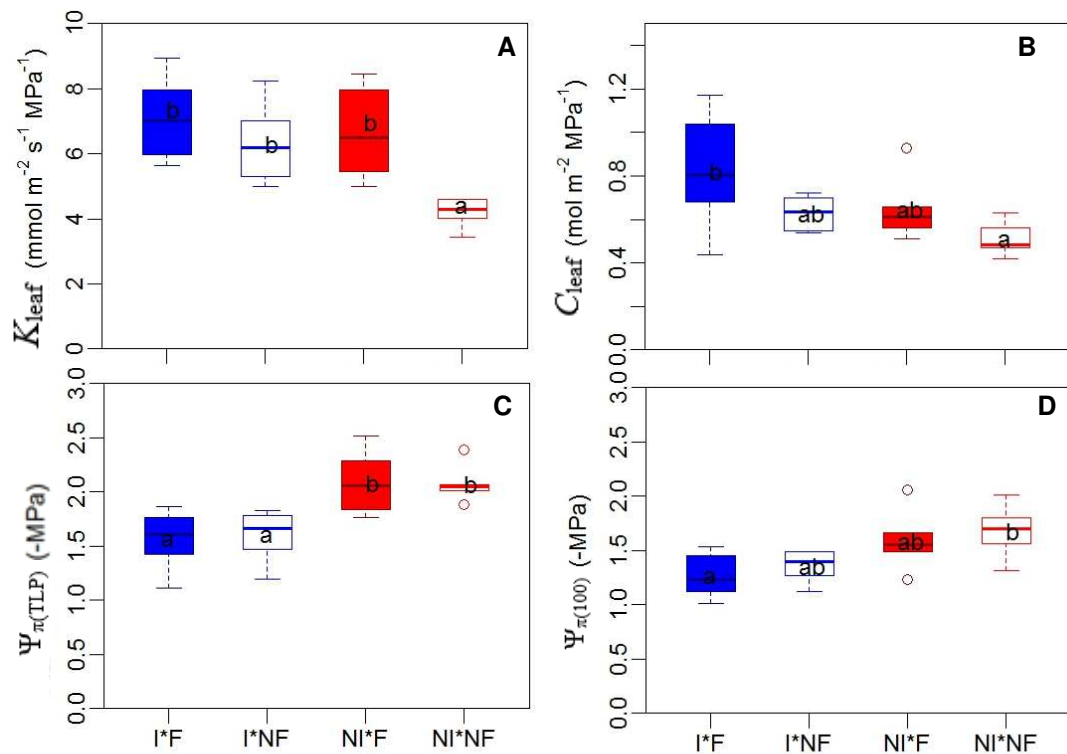
Fig. 6. A) Leaf hydraulic conductance (K_{leaf}), B) leaf capacitance (C_{leaf}), C) osmotic potential at the turgor loss point ($\Psi_{\pi(TLP)}$), and D) osmotic potential at full turgor ($\Psi_{\pi(100)}$) in *Coffea arabica* expanding leaves trees grown in the field and subjected to four treatment combinations: irrigated plants with fruits (I*F); irrigated plants with no fruits (I*NF); non-irrigated plants with fruits (NI*F) and non-irrigated plants with no fruits (NI*NF) ($n = 6$). The xth percentile is the value below which x % of the observations are found. The lower and the higher part of the box indicate the 25th and 75th percentiles, respectively. The value of the bars are the 5th and the 95th percentile, and the 50th percentile (median) is given by the horizontal line within the box. Different letters indicate significant differences among between treatments, according to the Tukey HSD test, $p < 0.05$.
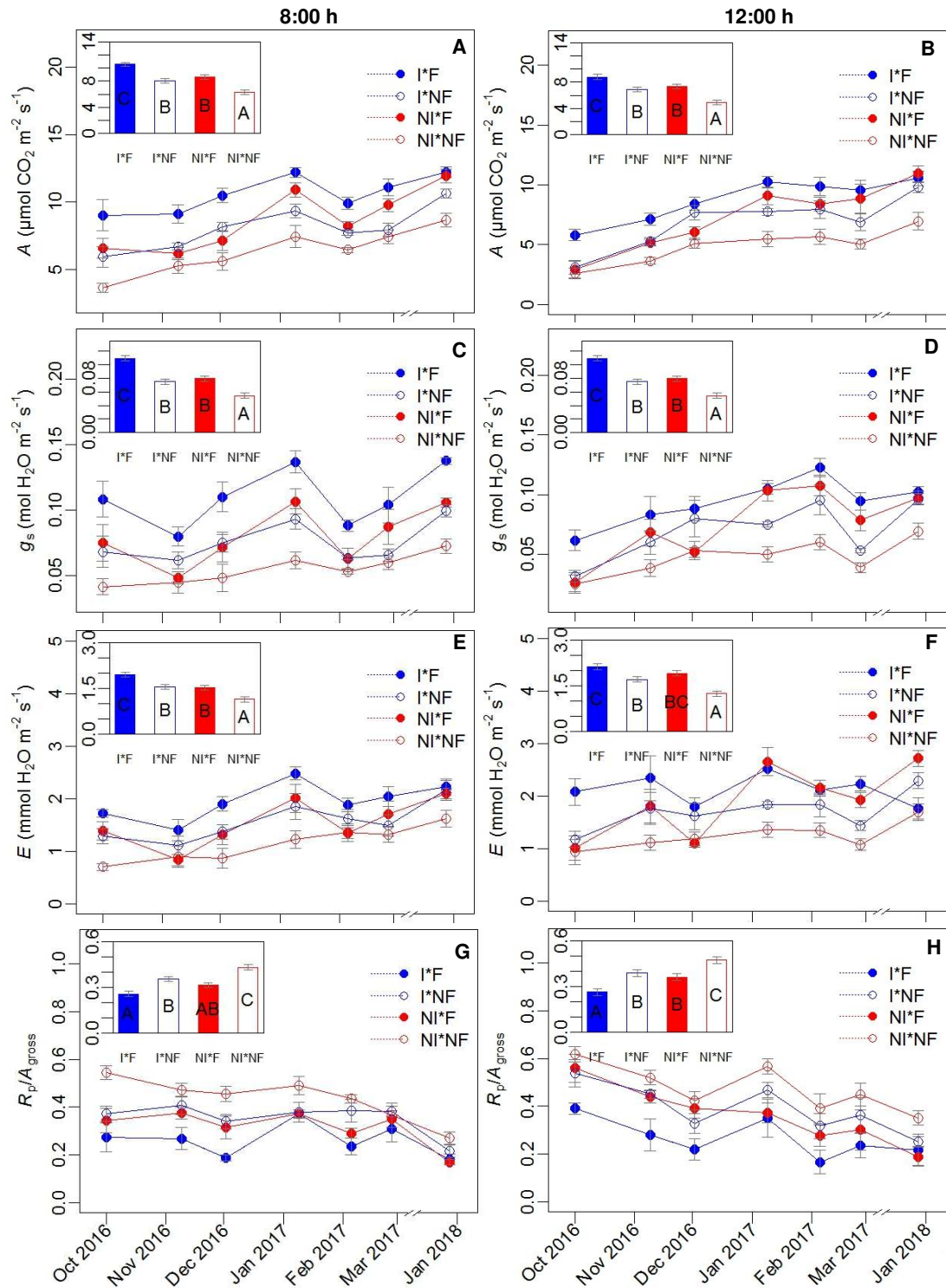
Fig. 7. Time course of A, B) the net CO_2 assimilation rate, A; C, D) stomatal conductance, g_s; E, F) transpiration rate, E, at 8:00h (left) and 12:00h (right) and G, H) the photorespiration-to-gross photosynthesis ratio, R_P/A_{gross} in *Coffea arabica* trees grown in the field and subjected to four treatment combinations: irrigated plants with fruits (I*F); irrigated plants with no fruits (I*NF); non-irrigated plants with fruits (NI*F) and non-irrigated plants with no fruits (NI*NF), at 8:00h (left) and 12:00h (right) from October 2016 through January 2018. Each data point represents the mean value ($n = 6 \pm SE$). Vertical bars denote SE; when not shown, the SE was smaller than the symbols. In the insets, mean values over the course of the
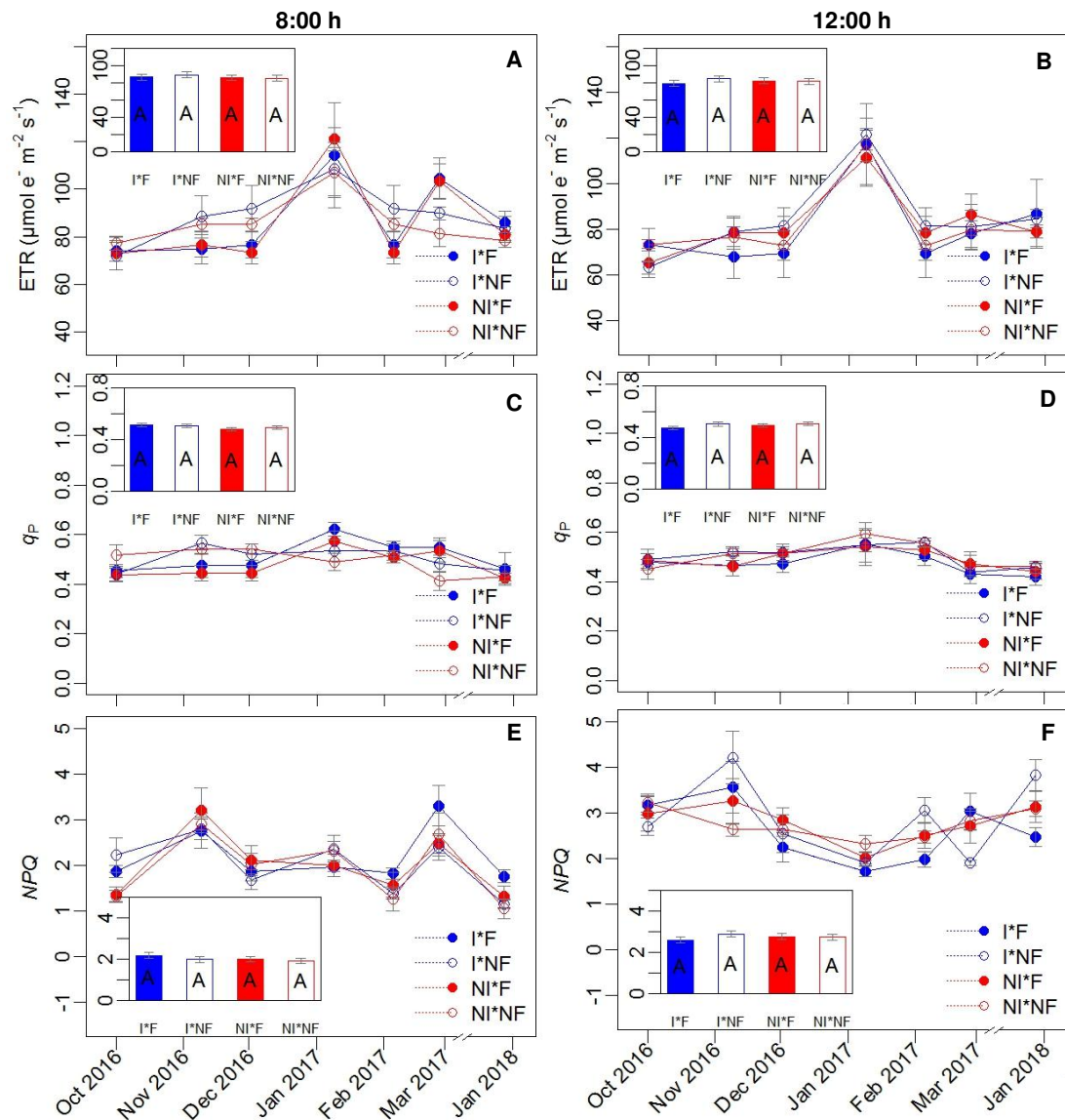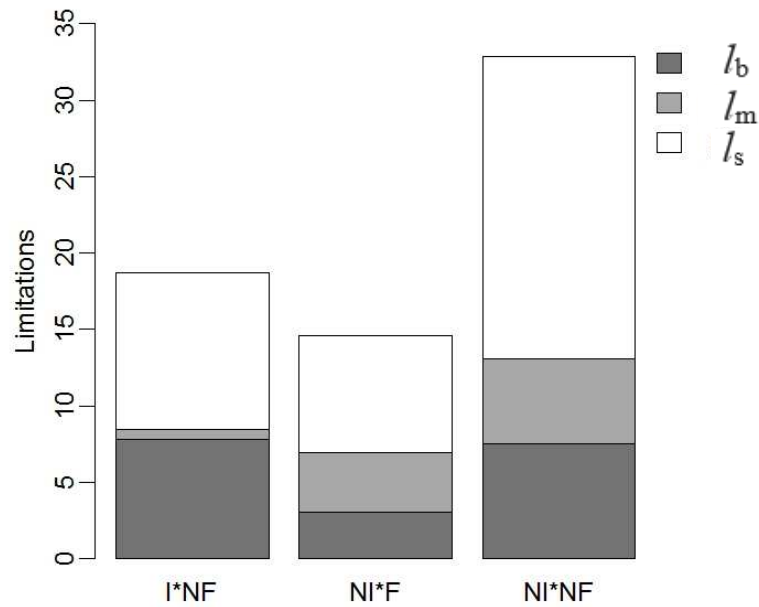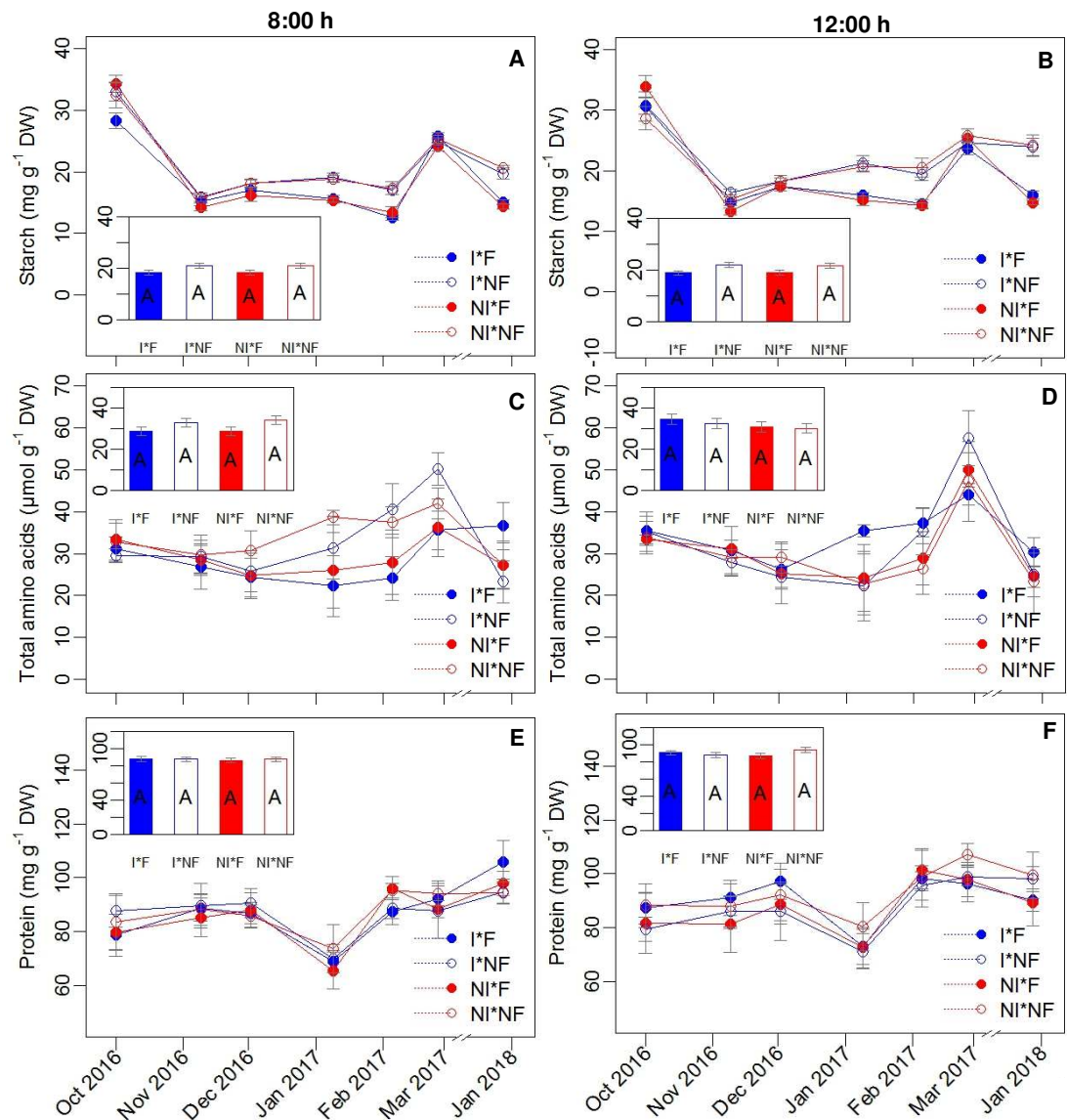
Supplementary Fig. 3. Time course of A, B) electron transport rate, ETR; C, D) photochemical quenching coefficient, q_P; and E, F) no photochemical quenching coefficient, NPQ, in *Coffea arabica* trees grown in the field and subjected to four treatment combinations: irrigated plants with fruits (I*F); irrigated plants with no fruits (I*NF); non-irrigated plants with fruits (NI*F) and non-irrigated plants with no fruits (NI*NF), at 8:00h (left) and 12:00h (right) from October 2016 through January 2018. Each data point represents the mean value ($n = 6 \pm$ SE). Vertical bars denote SE; when not shown, the SE was smaller than the symbols. In the insets, mean values over the course of the experiment are shown. Different letters indicate significant differences among between treatments, according to the Tukey HSD test, $p < 0.05$.
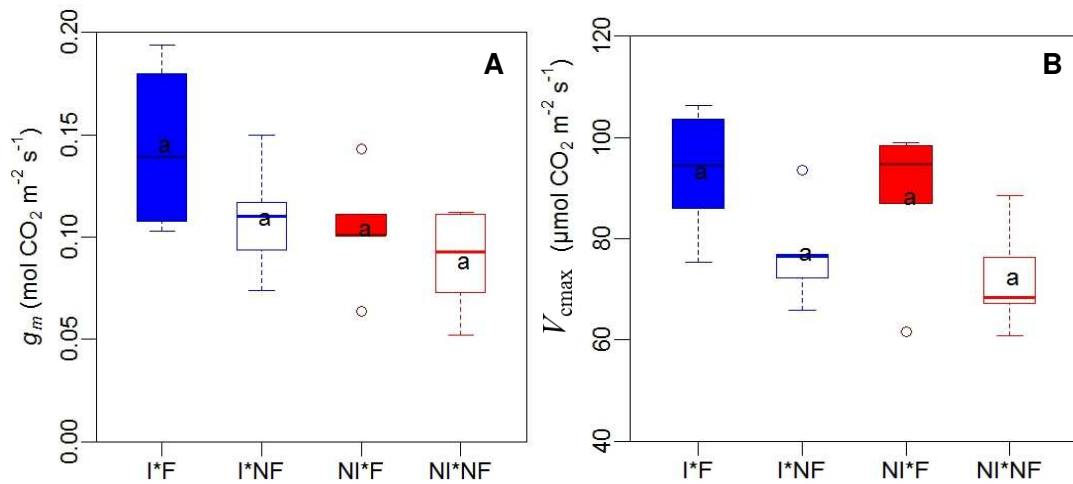
Fig. 8. A) Mesophyll conductance to CO_2 (g_m) and B) maximum rate of carboxylation by RuBisCO (V_{cmax}) based on a chloroplastic CO_2 concentration (C_c) in *Coffea arabica* trees grown in the field and subjected to four treatment combinations: irrigated plants with fruits (I*F); irrigated plants with no fruits (I*NF); non-irrigated plants with fruits (NI*F) and non-irrigated plants with no fruits (NI*NF) ($n = 6$). The xth percentile is the value below which x % of the observations are found. The lower and the higher part of the box indicate the 25th and 75th percentiles, respectively. The value of the bars are the 5th and the 95th percentile, and the 50th percentile (median) is given by the horizontal line within the box. Different letters indicate significant differences among between treatments, according to the Tukey HSD test, $p < 0.05$.

Fig. 9. Quantitative limitation analysis of photosynthetic CO_2 assimilation in *Coffea arabica* trees grown in the field and subjected to four treatment combinations: irrigated plants with fruits (I*F); irrigated plants with no fruits (I*NF); non-irrigated plants with fruits (NI*F) and non-irrigated plants with no fruits (NI*NF). The percentage of stomatal (l_s), mesophyll (l_m) and biochemical (l_b) limitations are shown relative to the I*F plants which displayed the greatest values of both net CO_2 assimilation rate (A) and stomatal conductance (g_s) ($n = 6$).
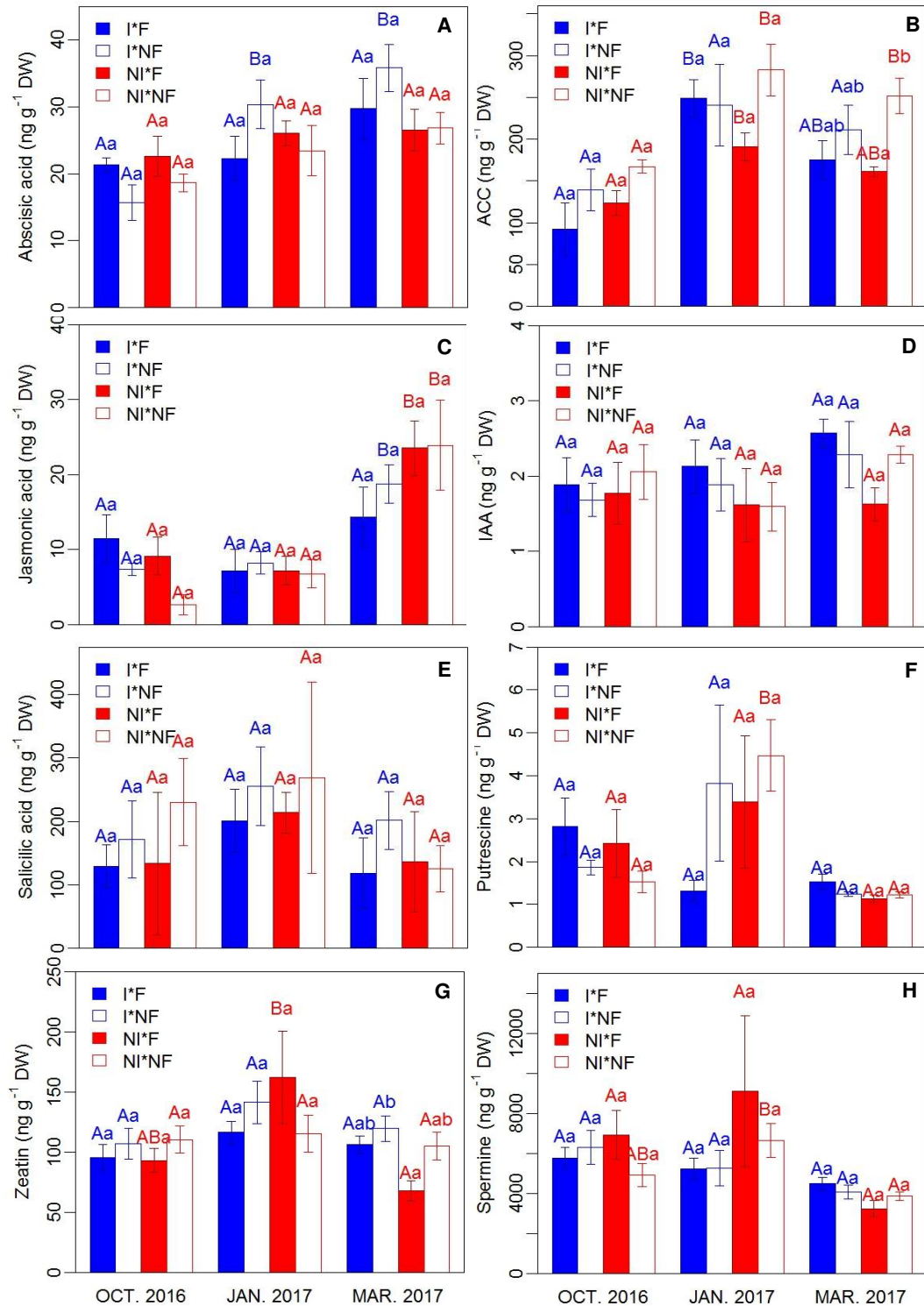
Supplementary Fig. 4. Time course of A, B) starch; C, D) total amino acids and E, F) protein in *Coffea arabica* trees grown in the field and subjected to four treatment combinations: irrigated plants with fruits (I*F); irrigated plants with no fruits (I*NF); non-irrigated plants with fruits (NI*F) and non-irrigated plants with no fruits (NI*NF), at 8:00h (left) and 12:00h (right) from October 2016 through January 2018. Each data point represents the mean value ($n = 6 \pm$ SE). Vertical bars denote SE; when not shown, the SE was smaller than the symbols. In the insets, mean values over the course of the experiment are shown. Different letters indicate significant differences among between treatments, according to the Tukey HSD test, $p < 0.05$.
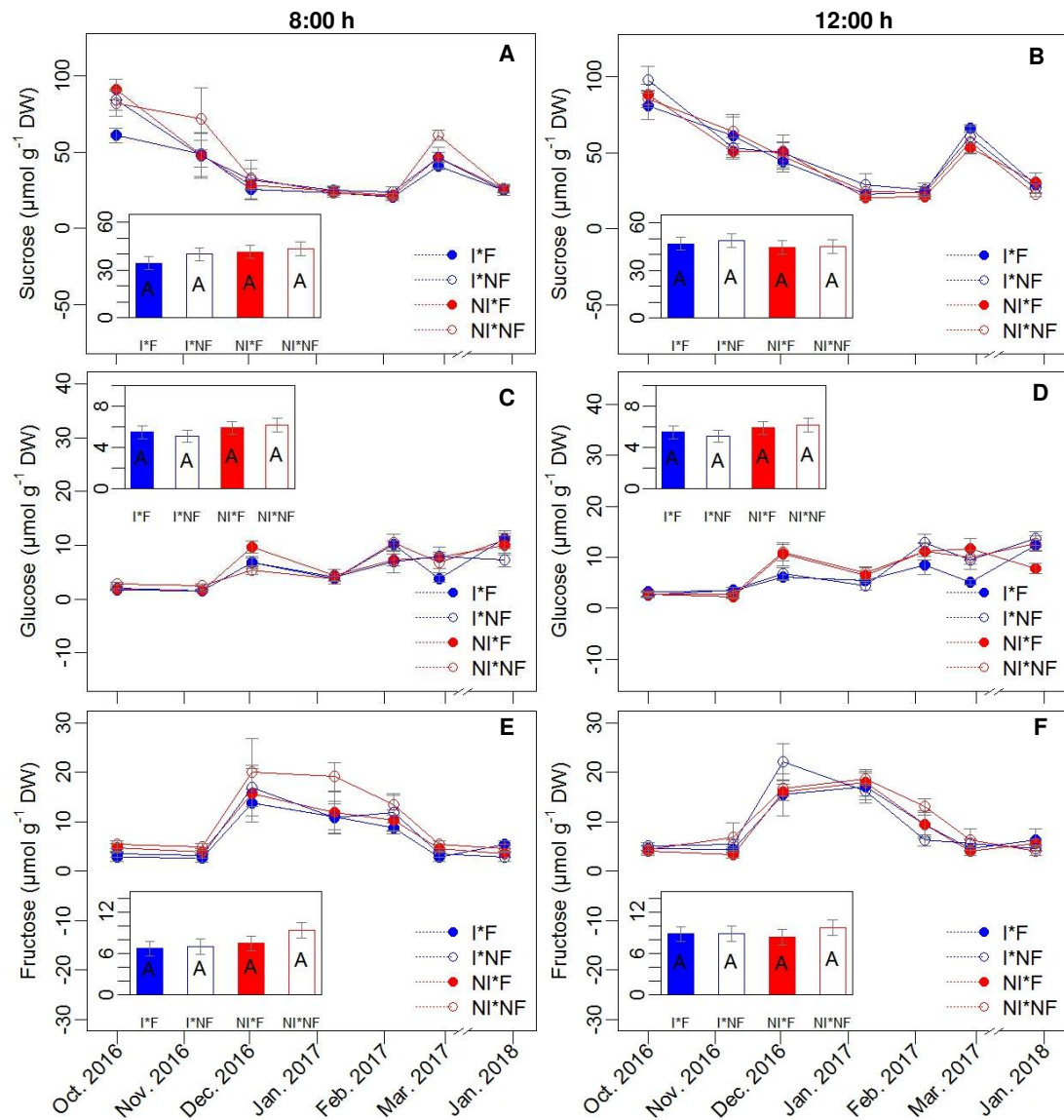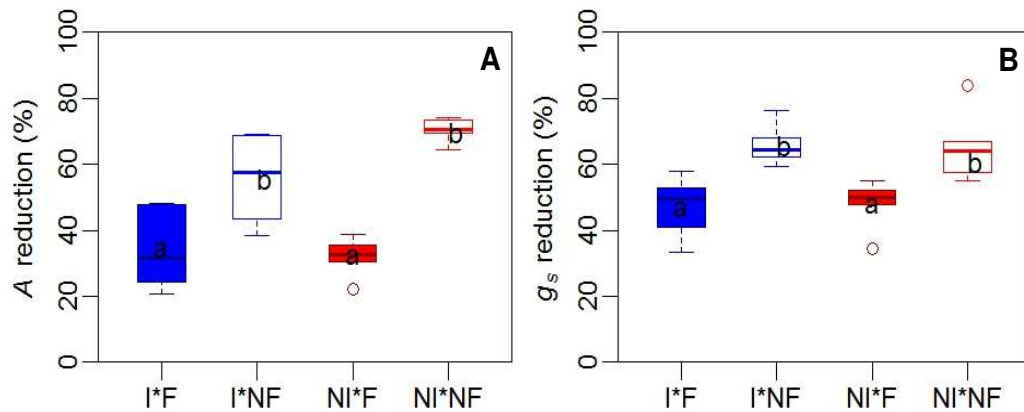
Supplementary Fig. 5. Time course of A, B) sucrose; C, D) glucose and E, F) fructose in *Coffea arabica* trees grown in the field and subjected to four treatment combinations: irrigated plants with fruits (I*F); irrigated plants with no fruits (I*NF); non-irrigated plants with fruits (NI*F) and non-irrigated plants with no fruits (NI*NF), at 8:00h (left) and 12:00h (right) from October 2016 through January 2018. Each data point represents the mean value ($n = 6 \pm SE$). Vertical bars denote SE; when not shown, the SE was smaller than the symbols. In the insets, mean values over the course of the experiment are shown. Different letters indicate significant differences among between treatments, according to the Tukey HSD test, $p < 0.05$.
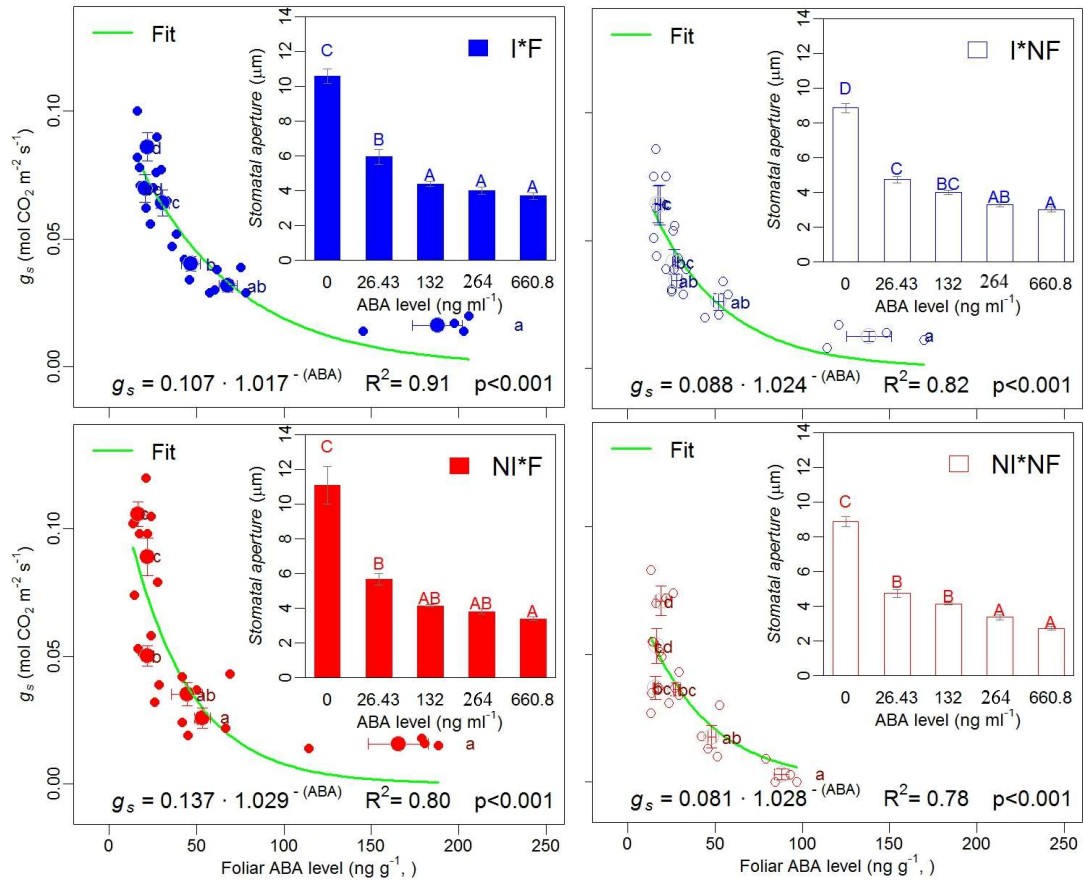
Supplementary Fig. 6. Hormonal profile [A) Abscisic acid, B) 1-aminocyclopropane-1-carboxylic acid (ACC), C) jasmonic acid, D) indole-3-acetic acid (IAA) E) salicylic acid, F) putrescine, G) Zeatin, H) spermine] of mature leaves from *Coffea arabica* trees grown in the field and subjected to four treatment combinations: irrigated plants with fruits (I*F); irrigated plants with no fruits (I*NF); non-irrigated plants with fruits (NI*F) and non-irrigated plants with no fruits (NI*NF) in October 2016 and in January and March 2017 ($n = 5 \pm$ SE). Different lowercase letters indicate differences between the treatment means within each time

point; different uppercase letters indicate differences over time. The means were compared using the Tukey test at $p < 0.05$.

Fig. 11. Reduction percentage of A) the net CO_2 assimilation rate, A; B) stomatal conductance, g_s following a VPD transition from 1.0 to 2.4 kPa in *Coffea arabica* trees grown in the field and subjected to four treatment combinations: irrigated plants with fruits (I*F); irrigated plants with no fruits (I*NF); non-irrigated plants with fruits (NI*F) and non-irrigated plants with no fruits (NI*NF) ($n = 6$). The xth percentile is the value below which x% of the observations are found. The lower and the higher part of the box indicate the 25th and 75th percentiles, respectively. The value of the bars are the 5th and the 95th percentile, and the 50th percentile (median) is given by the horizontal line within the box. Different letters indicate significant differences among between treatments, according to the Tukey HSD test, $p < 0.05$.

Fig. 12. The response of stomatal conductance (g_s) to exogenously applied abscisic acid (ABA) with fitted four-parameter exponential decay functions (green lines) and stomata aperture dimensions of isolated epidermis that were incubated with ABA at various concentrations (the inset in A-D depict stomatal aperture measurements of n = 100 viable stomata; mean ± SE). Vertical bars denote SE; when not shown, the SE was smaller than the symbols. Different letters indicate significant differences among between treatments, according to the Tukey HSD test, $p < 0.05$.